

**BOND STRENGTH OF EXTRUDED KAOLINITE BY  
TRIAxIAL EXTENSION TESTING**

By  
**ANNE-GRETHER TOPSHOJ**

**A THESIS PRESENTED TO THE GRADUATE COUNCIL OF  
THE UNIVERSITY OF FLORIDA  
IN PARTIAL FULFILLMENT OF THE REQUIREMENTS FOR THE  
DEGREE OF MASTER OF SCIENCE IN ENGINEERING**

**UNIVERSITY OF FLORIDA**

**1970**

## ACKNOWLEDGEMENTS

The writer wishes to thank all the persons who have helped with suggestions and assistance for the performance of the test series and the writing of this thesis.

Particularly the writer is grateful to the Chairman of the Supervisory Committee, Professor John H. Schmertmann, for his interest and help in the investigation.

Grant No. GK-1908X from the National Science Foundation made this work possible financially. Using this grant, the Department of Civil Engineering awarded the writer a Graduate Research Assistantship.

LIST OF TABLES

TABLE		PAGE
1	Plan for test series I . . . . .	3
2	Plan for test series II and III . . . . .	3
3	Results from test series I . . . . .	36
4	Water contents, degrees of saturation and void ratios from test series I samples . . . .	42
5	Results from test series II . . . . .	56
6	Water contents, degrees of saturation and void ratios from test series II samples . . . .	64
7	The "cohesion" intercept from test series III. .	76
8	Results from test series III . . . . .	77
9	Water contents, degrees of saturation and void ratios from test series III samples . . . .	79
10	Summary of the measured bond strengths from this investigation . . . . .	80

TABLE OF CONTENTS

	PAGE
ACKNOWLEDGEMENTS . . . . .	ii
LIST OF TABLES . . . . .	vi
LIST OF FIGURES . . . . .	vii
NOTATION . . . . .	x
ABSTRACT . . . . .	xv
CHAPTER	
1 INTRODUCTION . . . . .	1
Purpose . . . . .	1
Scope . . . . .	2
2 TRIAXIAL AXIAL EXTENSION TESTS . . . . .	4
Review of method . . . . .	4
Previous use of extension tests . . . . .	7
3 SOIL AND EQUIPMENT USED IN THIS WORK . . . . .	10
Soil . . . . .	10
Soil characteristics . . . . .	11
Preparation of specimens . . . . .	11
Equipment . . . . .	13
Need for hanger system . . . . .	15
4 SERIES I - IDS TESTS . . . . .	18
Philosophy . . . . .	18
Performance of IDS test . . . . .	21
Review of previous work . . . . .	23

	PAGE
Set up of extension test samples . . . . .	25
Consolidation . . . . .	29
IDS testing . . . . .	29
Experimental results . . . . .	31
Water content, degree of saturation and void ratio . . . . .	34
Conclusions . . . . .	35
5 SERIES II - TESTS ON TENSION SAMPLES . . . . .	45
Introduction . . . . .	45
Previous work . . . . .	45
Theoretical tension limit . . . . .	46
Set up of tension samples . . . . .	47
Consolidation . . . . .	48
The tension tests . . . . .	48
Experimental results . . . . .	50
Water content, degree of saturation and void ratio . . . . .	57
Distribution of strain . . . . .	58
Distribution of water content . . . . .	59
Conclusions . . . . .	59
6 SERIES III - STRESS-DILATANCY TESTS . . . . .	65
Introduction . . . . .	65
Theory . . . . .	65
Set up of samples . . . . .	69
Consolidation . . . . .	69
Performance of tests . . . . .	69
Experimental results . . . . .	72

	PAGE
Water content, degree of saturation and void ratio . . . . .	74
Conclusion . . . . .	74
7 RESUME OF RESULTS AND SUGGESTIONS FOR FUTURE RESEARCH . . . . .	81
Resume . . . . .	81
Suggestions for future research . . . . .	82
BIBLIOGRAPHY . . . . .	83
BIOGRAPHICAL SKETCH . . . . .	85

## LIST OF FIGURES

FIGURE		PAGE
1	Coulomb failure criterion . . . . .	5
2	Stresses in triaxial compression and extension tests . . . . .	6
3	Kaolinite . . . . .	10
4	Initial water content of specimens used in this research . . . . .	12
5	Triaxial equipment . . . . .	14
6	Hvorslev effective strength components . . . . .	20
7	I and D components . . . . .	22
8	Illustration of IDS test two stress-strain curves . . . . .	22
9	Punching of internal drain in sample . . . . .	26
10	Inserting of a wet, double wool yarn, internal drain . . . . .	26
11	Sample placed in 8 cm miter box and cut to 8 cm length . . . . .	27
12	Sample set on pedestal of triaxial appa- ratus, filter strips in place, ready for membrane cover . . . . .	27
13	Consolidation stage of test . . . . .	28
14	The I component as a function of the average effective stress, $\bar{\sigma}'_t$ at Mohr circle tangent point . . . . .	33
15	The D Component as a function of average effective stress . . . . .	37
16	Series I - pieces of constant-structure envelopes at $I_{\max}$ . Series II and III - $(\sigma_1 - \sigma_3)_{\max}$ points of Mohr circles . . . . .	38

FIGURE		PAGE
17	Example of stress-strain curve from IDS tests, overconsolidated specimen . . . . .	39
18	Example of stress-strain curve from IDS tests, normally consolidated specimen . . . . .	40
19	Example of the I and D component as a function of vertical strain for a normally consolidated specimen . . . . .	41
20	Example of the I and D component as a function of vertical strain for an overconsolidated specimen . . . . .	41
21	The final void ratio . . . . .	43
22	The void ratio after consolidation . . . . .	44
23	Sketch of tension specimen with dimensions . . . . .	49
24	Trimming of tension sample with reduced middle section . . . . .	51
25	Performance of test in test series II . . . . .	51
26	Sample with failure planes and heads of straight pins . . . . .	52
27	$(\sigma_1 - \sigma_3)_{\max}$ as a function of $(\sigma_1' + \sigma_3')$ before stress-dilatancy correction . . . . .	54
28	$(\sigma_1 - \sigma_3)_{\max}$ as a function of the void ratio at end of test for entire sample . . . . .	54
29	$(\sigma_1 - \sigma_3)_{\max}$ as a function of $(\sigma_1' + \sigma_3')$ after an approximate stress-dilatancy correction. . . . .	55
30	Distribution of vertical strain after test by measuring pin spacings on opposite sides of sample after test . . . . .	61
31	Initial and final water content of specimen . . . . .	62
32	Example of stress-strain curve from test series II . . . . .	63
33	Volume measuring device used in stress-dilatancy tests . . . . .	70



FIGURE

PAGE

34	Stress paths for test series III with stress-dilatancy correction . . . . .	75
35	Example of stress-strain curve from test series III . . . . .	78

## NOTATION

a	constant, see page 54
A	cross section area of specimen
A <sub>O</sub>	area of specimen after consolidation phase
A <sub>C</sub>	area of end sections of the tension sample
A <sub>E</sub>	area of reduced center section of the tension sample
A <sub>P</sub>	cross section area of the piston
c	cohesion term in Coulomb's equation
c <sub>e</sub>	Hvorslev effective or "true" cohesion
c <sub>f</sub>	cohesion corrected for stress-dilatancy
C.I.	confidence interval
$d = \frac{D}{\sigma_t}$	slope of constant-structure envelope
D	effective stress Dependent component of mobilized shear resistance
e	void ratio of specimen
e <sub>i</sub>	initial void ratio
e <sub>cons</sub>	void ratio after consolidation phase
e <sub>f</sub>	final void ratio
G <sub>s</sub>	specific gravity of soil solids
h	height of specimen

I	effective stress Independent component of mobilized shear resistance
$I_0$	bond strength
$I_{max}$	maximum value of I component in a test
$K = \frac{\sigma_1}{\sigma_3}$	ratio of principal stresses during consolidation phase
K	constant, see page 20
$K_1$	constant, see page 16
$K_{pf}$	$= \tan^2 (45^\circ + \frac{\phi_f}{2})$
LI	$= \frac{w-PL}{LL-PL}$ , liquidity index
LL	Atterberg liquid limit
n	number of observations used in regression analysis
P	uplift on piston
PI	plasticity index
PL	Atterberg plastic limit
s	$= c + \sigma \tan \phi$ , shear strength in Coulomb's equation
S	degree of saturation
$S_i$	initial degree of saturation
$S_{cons}$	degree of saturation after consolidation phase
$S_f$	final degree of saturation
$t_{100}$	time to the end of primary consolidation
T	tensile force
u	pore water pressure
$u_{high}$	pore water pressure at $\sigma_1'$ high pressure level
$u_{low}$	pore water pressure at $\sigma_1'$ low pressure level

w	water content of specimen
w <sub>i</sub>	initial water content
w <sub>cons</sub>	water content after consolidation phase
w <sub>f</sub>	final water content
δE'	increment of energy per unit volume transmitted to soil element
δU	increment of internal stored elastic energy per unit volume
δv	increment of volumetric strain, defined δv > 0 for volume decrease, = 2δε <sub>1</sub> + δε <sub>3</sub> in extension tests
δW	increment of energy dissipated per unit volume in frictional heat loss
δε <sub>1</sub>	increment of major principal strain, defined δε <sub>1</sub> > 0 in compression
δε <sub>3</sub>	increment of minor principal strain, defined δε <sub>3</sub> > 0 in compression
Δh	increment of height of specimen, defined Δh > 0 for increase in height
Δσ <sub>1</sub> '	= σ <sub>1</sub> ' <sub>high</sub> - σ <sub>1</sub> ' <sub>low</sub> , difference in major principal effective stress in the IDS test
ε	strain
ε <sub>1</sub>	strain in the same direction as σ <sub>1</sub> , defined ε <sub>1</sub> > 0 in compression = vertical strain in compression test
ε <sub>3</sub>	strain in the same direction as σ <sub>3</sub> , defined in this paper σ <sub>3</sub> > 0 in extension = vertical strain in extension tests
ε <sub>v</sub>	volumetric strain, defined in this paper ε <sub>v</sub> > 0 for volume increase
ε <sub>x</sub>	strain, see page 22
σ	= $\frac{\sigma_1 + \sigma_3}{2}$ , mean principal stress
σ <sub>1</sub>	major principal stress

$\sigma_2$	intermediate principal stress
$\sigma_3$	minor principal stress
$(\sigma_1 - \sigma_3)_{\max}$	maximum value of deviator stress
$\sigma_{\text{cons}}$	consolidation pressure
$\sigma_h$	hydrostatic cell pressure
$\sigma'$	$= \sigma - u$ , effective stress $= \frac{\sigma_1 + \sigma_3}{2}$
$\sigma'_1$	major principal effective stress
$\sigma'_{1 \text{ high}}$	major principal effective stress at high pressure level
$\sigma'_{1 \text{ low}}$	major principal effective stress at low pressure level
$\sigma'_2$	intermediate principal effective stress
$\sigma'_3$	minor principal effective stress
$\sigma'_{\text{cons}}$	effective consolidation pressure
Subscript "corr"	on $(\frac{\sigma_1}{\sigma_3})$ , $(\sigma'_1 + \sigma'_3)$ and $(\sigma_1 - \sigma_3)$ refers to values corrected for stress dilatancy
$\sigma'_C$	axial effective stress on the reduced center section of tension sample
$\sigma'_E$	average axial effective stress on the ends of tension samples
$\bar{\sigma}'_1$	$= 1/2 (\sigma'_{1 \text{ high}} + \sigma'_{1 \text{ low}})$ , average major principal effective stress
$\bar{\sigma}'_t$	average effective stress, at strain of $I_{\max}$ , between the two points of common Mohr circle tangency in an IDS test
$\tau$	$= 1/2 (\sigma_1 - \sigma_3)$ , shear stress

- $\phi$  angle of internal friction in Coulomb's equation
- $\phi_e$  Hvorslev effective or "true" angle of internal friction
- $\phi_f$  angle of internal friction corrected for stress-dilatancy
- $\psi$  constant, see page 54

Abstract of Thesis Presented to the Graduate Council  
in Partial Fulfillment of the Requirements for the  
Degree of Master of Science in Engineering

BOND STRENGTH OF EXTRUDED KAOLINITE BY  
TRIAXIAL EXTENSION TESTING

By

Anne-Grethe Topshoj  
June, 1970

Chairman: Professor John H. Schmertmann  
Major Department: Civil Engineering

This study investigates the bond strength of extruded kaolinite soil using axial extension tests, with bond strength defined as the shear strength of a dilatancy-free soil structure at zero effective stress.

Three test series were performed in a triaxial apparatus, each using a different principle to evaluate bond strength. First, the so-called IDS test was tried in extension; second, tension specimen tests were performed in the low range of effective lateral pressure and third, a series where conventional drained test data were corrected for stress-dilatancy and analyzed according to the methods of Rowe.

The IDS extension test results for bond strength gave good agreement with previous IDS compression tests. Each of the test series gave a bond strength as follows:

Test series I  $I_o = 0.084 \pm 0.025$  (kg/cm<sup>2</sup>)

Test series II  $I_o = 0.112 \pm 0.041$  (kg/cm<sup>2</sup>) before  
dilatancy correction

and  $I_o = 0.084 \pm 0.032$  (kg/cm<sup>2</sup>) after  
dilatancy correction

Test series III  $I_o = 0.117 \pm 0.552$  (kg/cm<sup>2</sup>)

## CHAPTER 1

### INTRODUCTION

#### Purpose

The purpose of this investigation is to measure the magnitude of the bond strength of a soil in axial extension tests, and to compare results from different methods. It is also a test of the IDS method in axial extension. Will it work? How do the results compare with the results in compression?

Part of the shear strength of a cohesive soil results from the internal bonding between the soil's particles. According to Webster's Dictionary bond means something that binds or restrains. Herein, the bond strength is defined as the shear strength of a dilatancy-free soil when the effective stress is zero. The bonding between clay particles is an important factor in the strength, and therefore engineering behavior of a soil.

The investigation is a continuation of work done by Professor John H. Schmertmann. The work is still in progress at the University of Florida under Professor Schmertmann's supervision. The previous work was, in part, also performed on extruded kaolinite soil samples.



## Scope

Three test series were run in this investigation in order to determine the bond strength of a soil. All tests were performed on the same clay soil, extruded kaolinite, and all as triaxial extension tests. Tables 1 and 2 present summaries of these tests as conducted in the three series. The plans were followed with minor deviations, and most of the tests were performed twice.

Test series I, IDS tests. - The IDS test is a special test technique developed by Schmertmann. Schmertmann generalized the Hvorslev effective components of shear resistance into the two components I and D. For this thesis work the test technique was tried in triaxial extension for the first time.

Test series II, tests on tension samples. - In this test series the author used a soil sample with smaller area at the center than at the ends. Using this shape of sample one can determine the shear resistance in the very low range of effective stresses. One can actually obtain negative effective stresses in the central, reduced area part of the soil sample without using clamping of the sample to the bottom or top caps.

Test series III, stress-dilatancy tests. - When the soil sample strains, work is done on or by the surroundings. The shear strength of soil can be separated into energy and fundamental components, using the concepts of Rowe. This series of extension tests used his methods to evaluate the kaolinite's bond strength.

Table 1. Plan for test series I

Consolidation			IDS Test	
	$\sigma_{\text{cons}}$ Initial Kg/cm <sup>2</sup>	$\sigma_{\text{cons}}$ Rebound Kg/cm <sup>2</sup>	$\sigma_1$ high Kg/cm <sup>2</sup>	$\sigma_1$ low Kg/cm <sup>2</sup>
Normally consolidated	6	6	5.70	4.50
	4	4	3.80	3.00
	3	3	2.85	2.25
	2	2	1.90	1.50
	1	1	0.95	0.75
	0.5	0.5	0.48	0.38
Over - consolidated	6	2	1.90	1.50
	4	2	1.90	1.50
	6	1	0.95	0.75
	4	1	0.95	0.75

Table 2. Plan for test series II and III

Test Series	Consolidation Kg/cm <sup>2</sup>	
II	Normally consoli- dated	0.1
		0.2
		0.3
		0.4
		0.5
III		1.0
		2.0
		4.0

## CHAPTER 2

### TRIAxIAL AXIAL EXTENSION TESTS

#### Review of method

There are many different types of strength tests that may be performed using the triaxial apparatus. Usually the test is divided into two stages. During the first stage a hydrostatic cell pressure is applied. Drainage may or may not be permitted. During the second stage an additional vertical deviator stress is applied until "failure" occurs. Usually the cell pressure is held constant during this stage. The soil sample is usually saturated with water, often with the aid of back pressure. Soil volume changes, if permitted, can then be observed during the test. Readings of deviator stress, pore pressure or volume change and vertical strain are taken throughout a test.

One way to indicate a soil's strength behavior is to plot the Mohr stress circle in a  $\tau, \sigma$  diagram, where  $\tau = \frac{\sigma_1 - \sigma_3}{2}$ . The radius of the circle is  $\frac{\sigma_1 - \sigma_3}{2}$  and the distance to its center from the origin along the  $\sigma$  axis is  $\frac{\sigma_1 + \sigma_3}{2}$ . A method of plotting the test results is to plot the top point of the Mohr circle. The locus of such points during a test forms a common type of stress path, also used herein.

Coulomb's criterion of failure is indicated by the following formula

$$s = c + \sigma \tan \phi \quad [1]$$

wherein  $c$  is called the cohesion,  $\phi$  the angle of internal friction, and  $s$  is the shear strength. The Coulomb criterion does not include any effects due to the intermediate principal stress  $\sigma_2$ . See Figure 1.

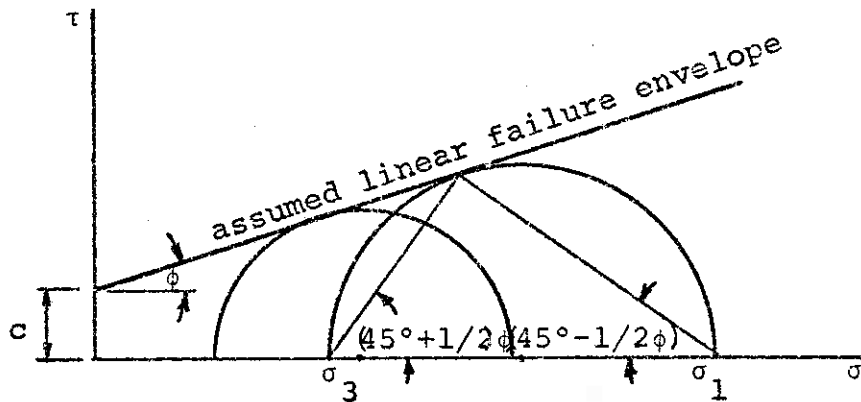


Figure 1. Coulomb failure criterion

For the compression test, the minor principal stress is the hydrostatic cell pressure  $\sigma_h$  and the major principal stress

is the cell pressure plus the deviator stress ( $\sigma_1 - \sigma_3$ )

$$\sigma_1 = \sigma_h + (\sigma_1 - \sigma_3) \quad [2]$$

For the extension test, the major principal stress is equal to the cell pressure  $\sigma_h$  and the minor is equal to the cell pressure minus the deviator stress. See Figure 2.

$$\sigma_3 = \sigma_h - (\sigma_1 - \sigma_3) \quad [3]$$

Clamping the soil sample to bottom and top cap is not necessary for the extension test so long as  $\sigma_3$  is positive, i.e. we do not really have tension in the soil, but we are only decreasing the compressive stress.

When presenting data in terms of effective stresses the effect of pore pressure  $u$ , if any, must be included

$$\sigma' = \sigma - u \quad [4]$$

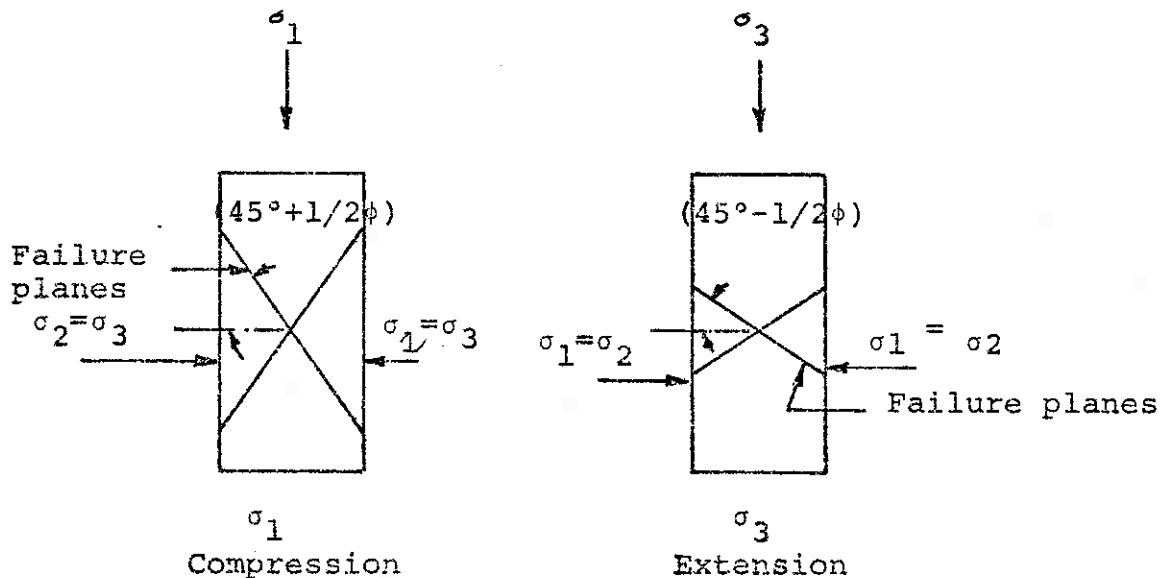


Figure 2. Stresses in triaxial compression and extension tests

### Previous use of extension tests

Much work has been done with triaxial extension tests. The test data are usually compared with those in compression tests, and agreement is not always found.

Roscoe (1)\* performed triaxial compression and extension tests on sand where he measured the local deformations, including both lateral and axial strains, during the test. He showed that the distribution of the deformation within the specimen is different for compression and extension tests, and the strains are nonuniform, especially for the extension test. He suggested that the results from the two types of test cannot be compared. However, total vertical strains were about 20% in these tests, which is at least five times the maximum strain in the present research.

Parry (2) performed a series of drained and undrained compression and extension triaxial tests on Weald clay. He found the Mohr effective stress failure envelope to be independent of test type and independent of overconsolidation ratio.

For extension tests he used spiral drains consisting of filter paper around each sample, and found that the rate of consolidation with spiral drains was half of that with vertical drains. He performed two types of extension tests: One, where radial stress is constant while axial stress decreases, and another, where radial stress increases while axial stress

---

\* Numbers in parentheses refer to the references listed on page 83.

is kept constant. This latter type of test is also known as an expansion test.

Constantino (3) performed compression, expansion and extension tests on granular soils. The first two series gave the same results, but the test results showed a quite different failure envelope for the extension tests. For the extension tests, the failure occurred near the ends of the specimen. Constantino suspected that the failure surface for those tests are curved, and that it was the reason for the different results. He was doubtful about the value of the extension test in granular soils.

One study by the U. S. Army Engineers (4) investigated the in situ properties of a saturated clay by triaxial tests. They found that triaxial extension generally decreases the  $(\sigma_1 - \sigma_3)_{\max}$  shear strength by 20%, increases the effective angle of friction, increases the stress-strain modulus, and increases the effective stress envelope for overconsolidated clays.

Ladd (5) investigated the stress-strain modulus of clay and found the modulus from triaxial extension tests several times higher than the modulus from compression tests.

Kirkpatrick (6) and Bishop (7) found the angle of friction for sand the same for extension and compression triaxial tests. If, however, stress-dilatancy correction is taken into account, Bishop found the values from the extension test much smaller. Kirkpatrick found the Coulomb failure criterion to be valid for sand in axial extension.

Habib (8) and Haythornthwaite (9) both report test series on sand and clay in compression and extension and note differences in the values from extension and compression tests. Haythornthwaite explained it by the non-uniformity of the stresses in a triaxial test sample. He abandons the Coulomb failure criterion and suggests an alternative yield criterion.



## CHAPTER 3

### SOIL AND EQUIPMENT USED IN THIS WORK

#### Soil

The tests reported herein were all performed on samples of machine extruded kaolinite clay. Kaolinite has some properties convenient for laboratory soil investigations. It has relatively high permeability compared to other clays, and when extruded by a "Vac-Aire" machine it gives a large number of duplicate soil samples with almost 100% saturation.

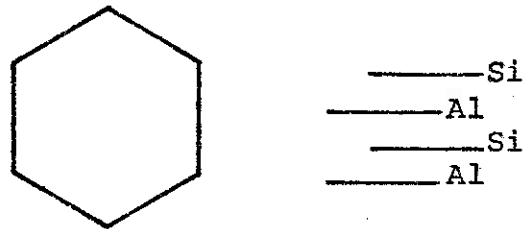


Figure 3. Kaolinite

The kaolinite clay mineral consists of silica and alumina sheets and most of its particles have a hexagonal shape, see Figure 3. Kaolinite is a very pure white clay with an earthy smell and a smooth and greasy feel.

The clay in our investigation was purchased about two years ago from Edgar Plastic Kaolin Company, Edgar, Florida. The plant was founded in 1892 and owned for many years by the Edgar family. Now it is owned by National Lead. Edgar is about 25 miles east of Gainesville. The clay in Edgar is mined, water washed, dried and pulverized and sold in 50 pound bags. It then consists of about 99.6% kaolinite. The clay is an alluvium deposit, derived mainly from feldspar. It is deposited with sand, which the plant sells as concrete aggregate.

#### Soil characteristics

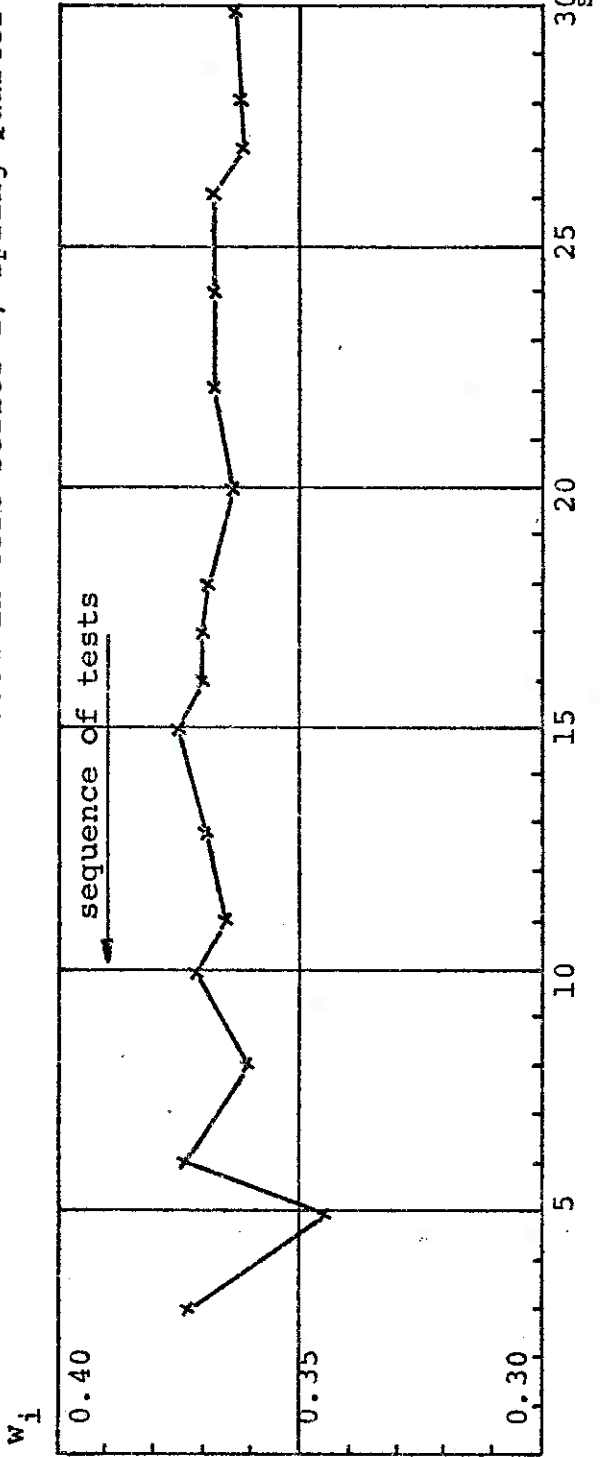
The clay had the following properties

Specific gravity, $G_s =$	2.609
Atterberg liquid limit, LL =	59.4%
Atterberg plastic limit, PL =	29.6%
Plasticity index, $PI = LL - PL =$	29.8
Water content, w =	37%
Liquidity index, $LI = \frac{w - PL}{LL - PL} = \frac{37 - 29.6}{29.8} =$	25.0%
Less than 0.002 mm	71%
Activity, $\frac{PI}{\%2w} = \frac{29.6}{71} =$	0.42

#### Preparation of specimens

The kaolinite was received in powdered form. The powdered kaolinite was mixed with distilled but not de-ionized water. The clay and water mixture was placed in a "Vac-Aire" extruding machine. The machine kneads and vacuums the air out of the

Batch I, extruded January 21, 1969  
 Used in test series I, Spring Quarter 1969



Batch II, extruded Summer 1969  
 Used in test series II and III, Fall Quarter 1969

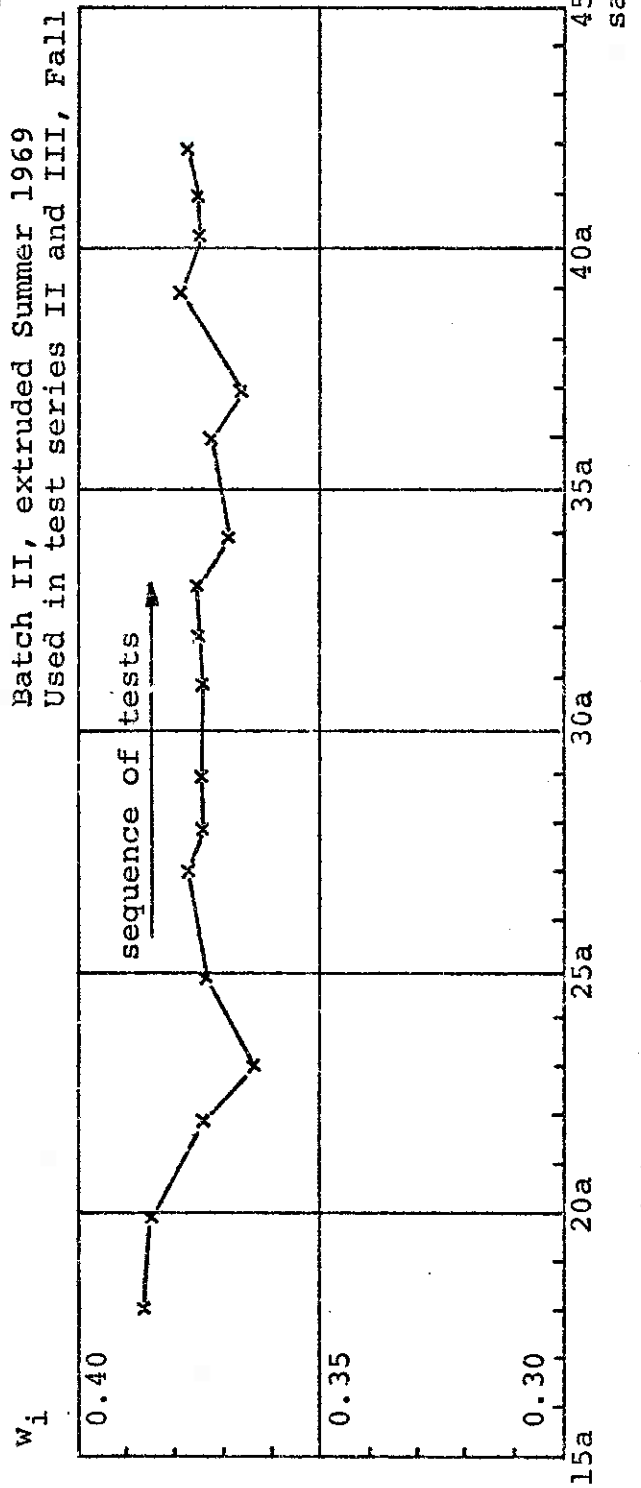


Figure 4. Initial water content of specimens used in this research

mixture and extrudes it in circular bars with a diameter of 3.58 cm. To help achieve a uniform product the clay was passed through the machine about five times. After the last time, the bars were cut into lengths of 10 cm and immediately wrapped in wax paper at least four times to avoid drying. The samples were wrapped in wax paper because the wax tends to stick to the clay. Successive numbers were placed on each specimen in the order they were extruded. Before testing, the sample height was reduced to eight centimeters. Three batches of clay samples were made during 1969, each batch containing about 50 specimens. In this investigation only samples from batches I and II were used.

The initial values of water content are shown in Figure 4. It is seen that batch II has a slightly higher water content than batch I, and that the water content decreases a little for increasing sample number, i.e. the last extruded specimens have lower water content.

### Equipment

There are many types of triaxial apparatus manufactured. Reference (10) describes the principal features of triaxial equipment. The triaxial apparatus used for this investigation was designed and manufactured at the Norwegian Geotechnical Institute, Norway (11). It was installed at the University of Florida about 1960.

Figure 5 gives an overall view of the triaxial section of the soil mechanics research laboratory and Figure 13 shows the triaxial cell used for this study.

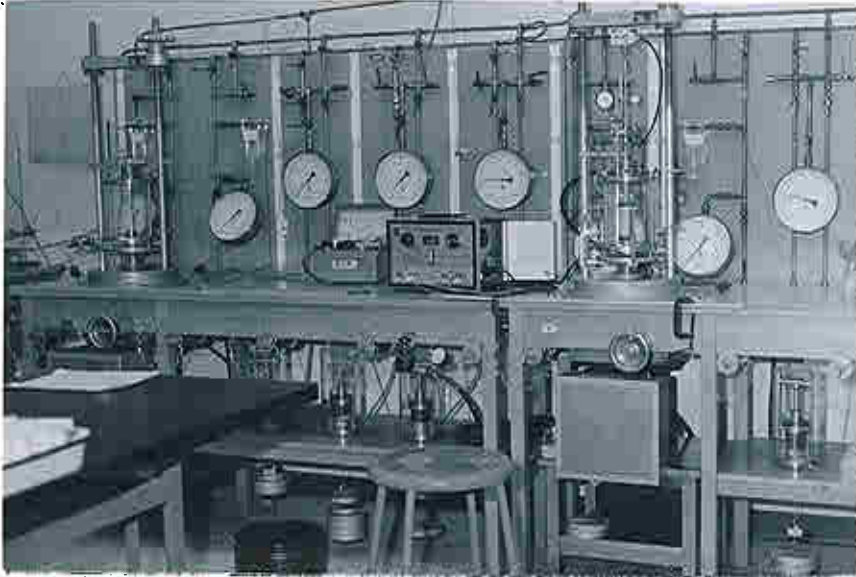


Figure 5. Triaxial equipment

Today there is much research and development in progress to get better and more accurate triaxial apparatus with, for example, completely eliminated piston friction, direct measurements of soil deformations, and the testing of much larger soil samples. The Norwegian apparatus does not include these advances but it is an older design of very high quality. It uses an oil-fed rotating bushing to decrease piston friction. Ordinarily the friction is negligible with this bushing.

Some modifications were made on the Norwegian apparatus in order to be able to perform extension tests. The piston was screwed into the top cap. Instead of the conventional proving ring, the deviator stress is measured by electrical units - a Thwing-Albert Load Cell connected through a bridge to a strain indicator. Its calibration was checked periodically and found reliable. Load sensitivity was about 0.0076 kg per division on the indicator, with readings reproducible to  $\pm 1$  division. To ensure accuracy in readings, one must also periodically check that all electrical connections are good.

#### Need for hanger system

Pressure in the triaxial cell causes uplift on the piston. This causes an uplift on the soil sample because the piston is screwed into the top cap.

The net uplift on the soil sample is a function of the cell pressure, the cross section area of the piston and the initial weight of the hanger system, piston and cap. The

uplift is

$$P = \sigma_h \cdot A_p - K_1 \quad [5]$$

$$A_p = 0.95 \text{ cm}^2 \quad [6]$$

where  $A_p$  is the cross area of the piston,  $\sigma_h$  the cell pressure and  $K_1$  the constant.

In the three test series reported herein, phase I of each test involved hydrostatic consolidation, i.e. same lateral as vertical pressure at mid-height of the soil sample. It is therefore necessary to apply a compensating load equal to the uplift  $P$  on the piston. For cell pressures from 0 to 2 kg/cm<sup>2</sup>, weights were put directly on the piston. For cell pressures over 2 kg/cm<sup>2</sup> the load was applied to a hanger system which has a lever arm ratio of 5, i.e. the load on the piston is five times the weight on the hanger.

For detailed information about the calibration work done to calibrate the load cell, volume measuring device, vertical strain versus movement of cell, hanger weight, effect of filter paper, constant pressure cell, mercury pot system, etc., see the original data sheets on file with Professor Schmertmann. The calibrations showed, among other things, that the vertical strain of sample is the same as the measured downward movement of cell, the filter drains placed on the samples do not seem to reinforce the specimen, and that tests number 301-321 were all performed with too much compensating hanger load.

The test results from these tests have been corrected for the mistake. The error caused these IDS tests to be consolidated

322 1st  
TENSION IN  
T.5

with  $K = \frac{\sigma_1}{\sigma_3}$  of about 1.02, which is only a minor deviation from hydrostatic pressure.



## CHAPTER 4

### SERIES I - IDS TESTS

#### Philosophy

The well known Hvorslev interpretation of the Coulomb failure criterion states that the shear strength of soil is equal to the effective cohesion  $c_e$  plus the effective stress multiplied by the tangent of the effective angle of friction  $\phi_e$

$$s = c_e + \sigma' \tan \phi_e \quad [7]$$

$c_e$  and  $\phi_e$  are also sometimes called the true strength components.

The true strength components of clay are seldom used in practical problems. They are important, however, for an understanding of the basic failure criteria.

Hvorslev demonstrated in 1937 that the effective or "true" angle of friction is a constant for a given clay, independent of the void ratio, and that the true cohesion is a function of the void ratio only. He showed that for two remolded, normally consolidated, clays the true shearing strength is proportional to the effective stress, i.e. that the Mohr failure circles for normally consolidated clay have a common tangent through the origin. Several investigators, however, claim

that many clays have an "origin cohesion." Hvorslev's ideas have been criticized by Rowe (12) and Schmertmann (13). The Hvorslev parameters are shown in Figure 6.

Professor John H. Schmertmann at the University of Florida has developed a special test technique which can be used to determine the effective stress Independent and effective stress Dependent components of a soil's mobilized shear resistance as a function of strain and at the same soil structure. A test employing this technique is called an IDS test. IDS stands for Independent and Dependent components as a function of Strain. At first the test was called the CFS test. CFS stands for Cohesion and Friction as a function of Strain. This notation was changed because in general  $I \neq c_e$  and  $D \neq \sigma' \tan \phi_e$ .

Schmertmann states that, in general, even though a clay has the same void ratio it does not necessarily mean equal soil structure and therefore equal cohesion, and that soil structure is a function of stress history, effective stress, strain and even time. He defines some more generalized components. First there is  $D$  = Dependent component, or the component of shear resistance mobilized at any plane and at any strain  $\epsilon$ , which is dependent on effective stress on that plane.

$$D = \sigma' d \quad [8]$$

Then there is  $I$  = Independent component, which is the remaining component defined by

$$I = \tau - D \quad [9]$$

The definitions of  $D$  and  $I$  are illustrated in Figure 7.

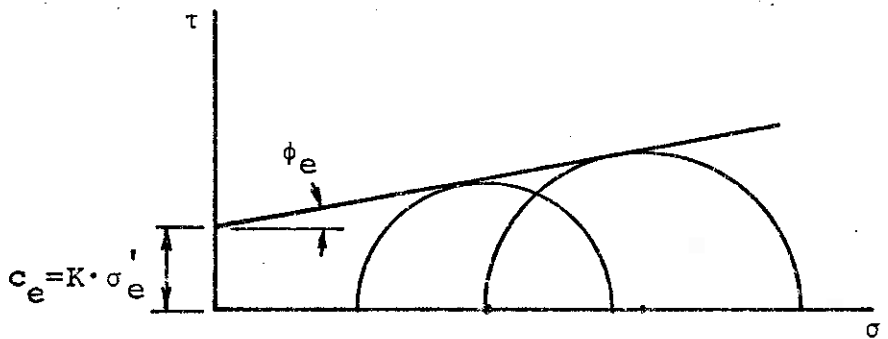


Figure 6. Hvorslev effective strength components

The  $c_e$  and  $\phi_e$  are determined from the common tangent as failure for two samples with same void ratio. One sample is normally consolidated and the other overconsolidated. Where  $\sigma_e$  = equivalent  $\sigma'$  on virgin curve corresponding to  $e$  of these samples.

Performance of IDS test

In the one specimen form of this test (14) only one specimen is used to obtain two stress-strain curves. In the constant  $-\sigma_1'$  form of the IDS test (15) the effective major principle stress  $\sigma_1'$  is varied by curve hopping back and forth between two constant values while the specimen is increasing in strain.

The pore pressure is usually controlled to maintain  $\sigma_1'$  as a constant.

$$\sigma_1' \text{ high} = \sigma_h - u \text{ high} \quad [10]$$

$$\sigma_1' \text{ low} = \sigma_h - u \text{ low} \quad [11]$$

$\sigma_1' \text{ high}$  and  $\sigma_1' \text{ low}$  are the two preselected values of the major principal stress. They are maintained constant by appropriately varying either cell or pore pressure. For the extension test  $\sigma_1'$  is the cell pressure less the pore pressure. Cell pressure was held constant and the pore pressure was varied to control  $\sigma_1'$  in the tests reported herein.

A curve hopping ratio  $\frac{\Delta \sigma_1'}{\sigma_{\text{cons}}}$  of 20% has been found convenient, with  $\sigma_1' \text{ high} = 95\%$  and  $\sigma_1' \text{ low} = 75\%$  of  $\sigma_{\text{cons}}$ . Figure 8 shows an illustration of the two stress-strain curves obtained with the curve hopping technique. After interpolation the I and D components can be separated at any strain, as shown in Figures 7 and 8.

It is important for test accuracy that the pore pressure be the same throughout the specimen. Internal wool drains

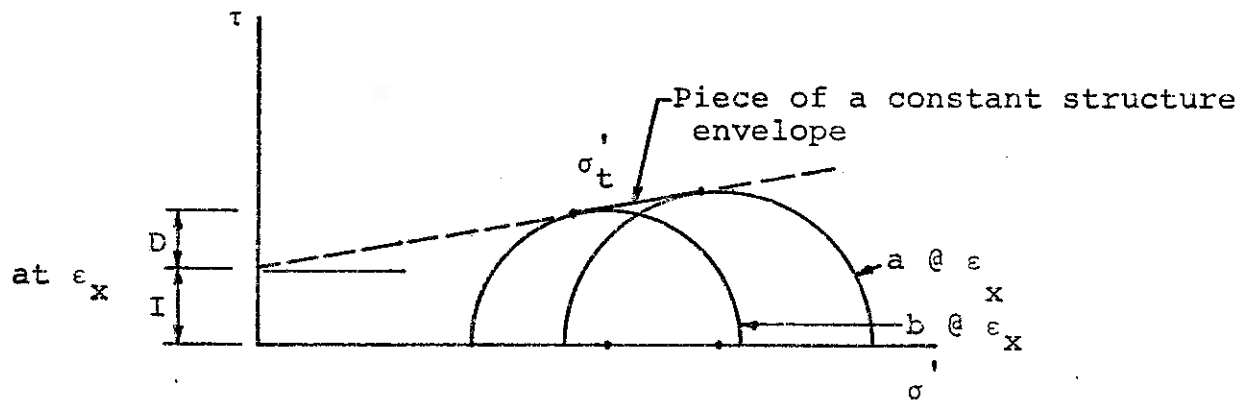


Figure 7. I and D components  
The components are determined from the common tangent at any strain  $\epsilon$

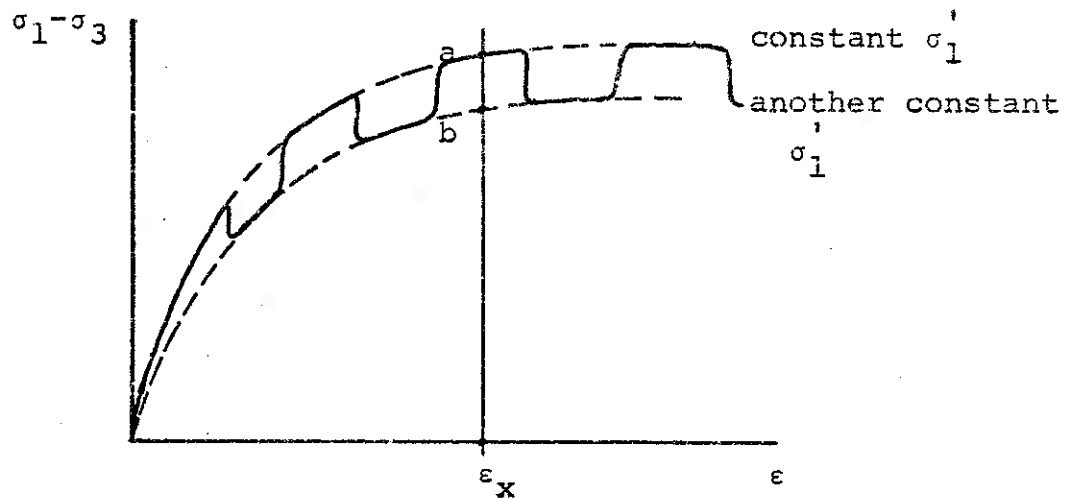


Figure 8. Illustration of IDS test  
two stress-strain curves with one specimen

and external filter paper strips aid achieving the desired pore pressure uniformity.

#### Review of previous work

Professor Schmertmann in one of his studies investigated the development of cohesion and friction with axial strain in saturated cohesive soils (15). Initially multiple-specimens were used. By refining test technique and method the one-specimen curve hopping technique was developed. One of the refinements was the use of internal wool drains to speed pore pressure dissipation. Another refinement was the use of a rigid load cell instead of a relatively flexible proving ring.

The results from this investigation showed that the measured I and D components act independently, with the maximum I developing at much lower strain than the maximum D and that the I component of a clay at a given water content is not a constant but is dependent on soil structure.

Schmertmann (14) has compared one-and two-specimen CFS tests. The investigation showed that the curve hopping technique with one specimen gives the same results as the tests with two specimens. Furthermore, it is recommended that the I and D components can be considered generalized Hvorslev strength components (14).

Schmertmann and John R. Hall (16) have studied the effect of non-hydrostatic consolidation on the I and D components. From the study it was concluded that the I component is unaffected by non-hydrostatic consolidation and the value of the D component is affected.

New data were applied and in an unpublished paper (17) Schmertmann presents the previous and the new data and discusses the concept of the I component. It is pointed out that the I component is a rather unique component of a soil's shear resistance. Also, the maximum value of the independent component  $I_{\max}$  is independent of other soil characteristics that are commonly considered as important to shear resistance, such as mineralogy, grain size distribution, soil structure and time effects.

To assist in defining bond strength Schmertmann introduced the concept of a constant-structure envelope, defined as a Mohr envelope which in terms of effective stress shows the maximum shear resistance that can be offered by a particular, constant soil structure. He then defines bond strength as the shear resistance of the soil when the constant-structure envelope intersects the I axis at zero effective stress. He further showed that this intercept and therefore bond could be determined by the I axis intersection of the locus of  $I_{\max}$  versus  $\bar{\sigma}'_t$  data.

The bond strengths for a silt, a cemented sand and several remolded and undisturbed clays were determined. Values fell between  $0.00 - 0.50 \text{ kg/cm}^2$  for the various soils.

Note that all of these previous data involve only axial compression tests. To the author's knowledge, the IDS test has not yet been used in extension testing.

Set up of extension test samples

After removal of the coating wax and the wax paper the soil sample was mounted in a 10 cm sample miter box. Three holes in a triangular pattern were punched vertically through the sample with a needle, 0.18 cm in diameter. Doubled wool yarn, saturated with water, was pulled through the prepunched holes. Figures 9 to 12 show some of the steps during the set up of these samples.

The sample was placed in an 8 cm sample miter box and cut to a length of 8 cm. The diameter remained at the extruded value of 3.58 cm. The sample was weighed and the height and diameter measured with a vernier calipers. Eight saturated filter strips were placed along the sides after the sample was mounted on the pedestal. Each filter strip was 7.6 cm in length and cut approximately 0.6 cm wide. The sample rests on a porous filter stone at the bottom but none at top. The filter strips touch the filter stone at the bottom.

Two Sheik rubber prophylactics, thickness 0.06 mm, were used as membranes to enclose the soil sample. Rubber sleeves were put on pedestal and top cap. A layer of Dow Corning 4 Compound silicone grease was used between rubber membranes and on rubber sleeves to ensure water tightness and two O-rings of unstretched inside diameter 3.1 cm were mounted on the pedestal and top cap to seal and hold the rubber membranes.

It is important to have all connections and tubes to the sample free from air bubbles. Before the set up of sample all tubes were flushed with de-aired water. The sample was set up as fast as possible to minimize drying.



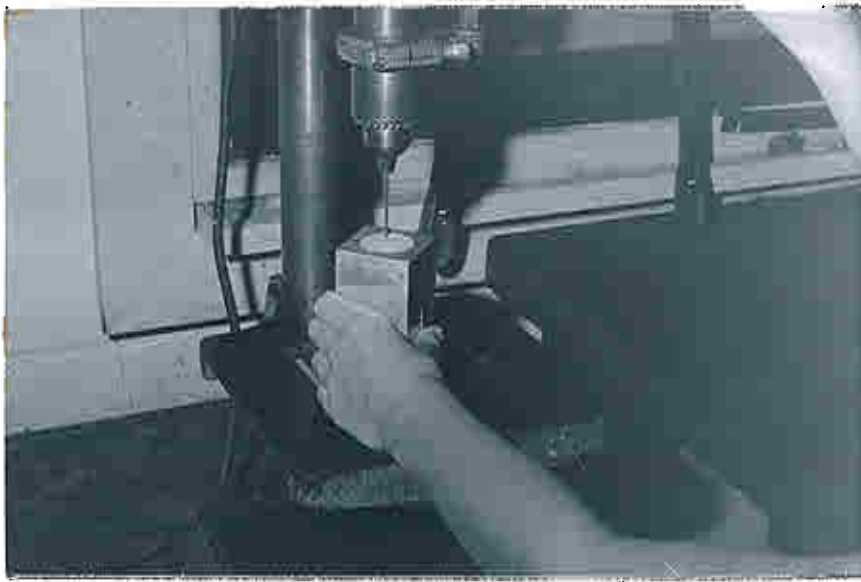


Figure 9. Punching of internal drain in sample



Figure 10. Insertion of a wet, double wool yarn, internal drain



Figure 11. Sample placed in 8 cm miter box and cut to 8 cm length

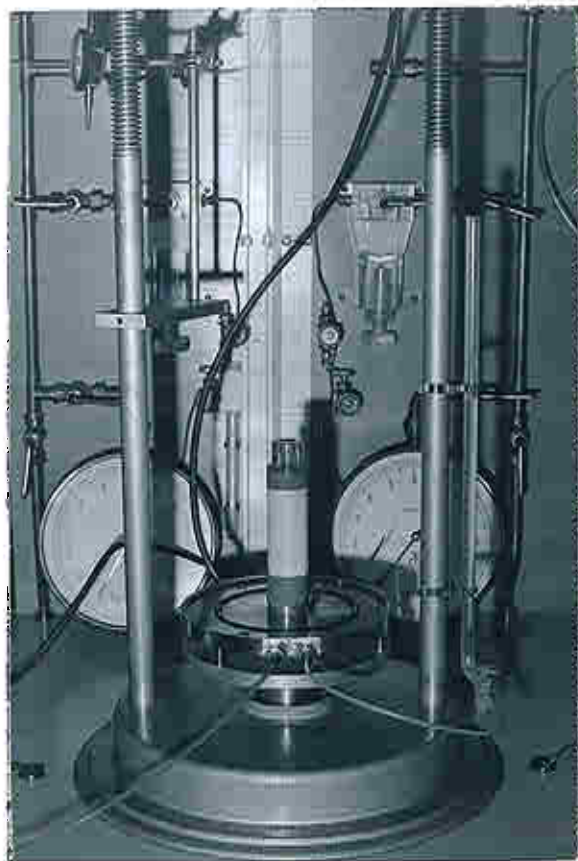


Figure 12. Sample set on pedestal of triaxial apparatus, filter strips in place, ready for membrane cover

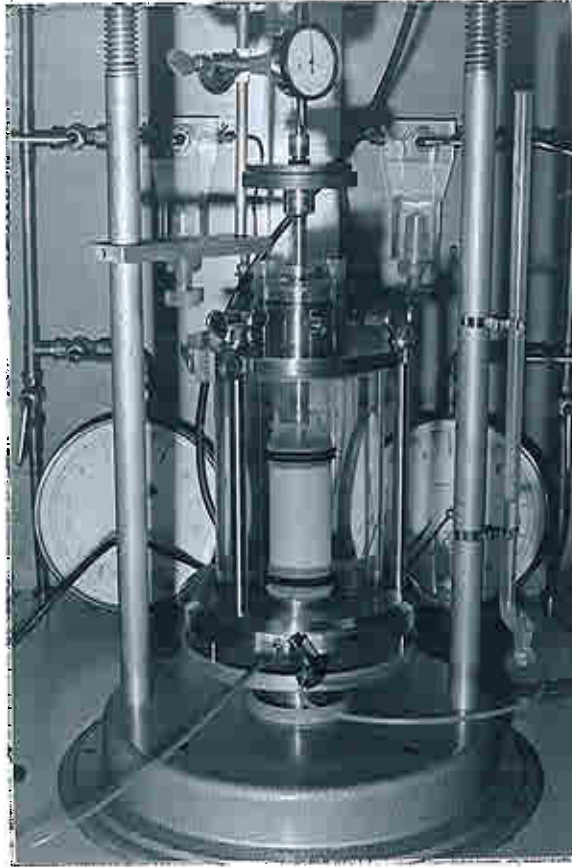


Figure 13. Consolidation stage of test  
(note the compensating weights directly on the  
piston and the piston screwed into top cap)

### Consolidation

Figure 13 shows one test during its consolidation stage. The cell pressure and the compensating weights on the hanger system were applied simultaneously. The volume change during consolidation was read on a burette with 0.1 ml divisions and without the use of back pressure. Volume change and vertical strain as a function of time were recorded and plotted in a semi-log graph.

The time to the end of primary consolidation,  $t_{100}$ , was found to be from 45 to 85 minutes using the Casagrande slope intersection method. Although much care was taken in avoiding air in the closed system, there were usually air bubbles coming out during consolidation. The major part of the undesirable air was probably trapped between the soil sample and the rubber membranes.

The soil sample was usually consolidated overnight for a total time of about 20 hours. As noted on page 16, the tests were consolidated with  $K = 1.02$ .

### IDS testing

Back pressure is important to ensure more complete saturation of the soil specimen and the connecting lines, valves, etc. A back pressure of 2, 3 or 4  $\text{kg/cm}^2$  was used in this test series. When applying back pressure the cell pressure and the hanger weight must be increased to higher values to keep the effective stress the same as the previous consolidation pressure.

The cell and back pressure were held by two different hydraulic constant-pressure cells. Two motors were kept running during test so that their vibrations could decrease friction in the constant-pressure cells. The triaxial cell was fastened to the movable load platform with three clamps. Simultaneous values of vertical strain, volume change and vertical load were recorded and rough plotted during each test.

These tests were all extension tests. The whole cell moves down with the load platform at a constant rate while the piston remains fixed to the load cell measuring the deviatoric piston tension.

The series I tests were performed with a rate of strain of approximately 1/2% per hour for normally consolidated clay and 1/3% per hour for overconsolidated clay. Slower speed was used for overconsolidated clay to permit better pore pressure equilibrium during the larger volume changes.

The cell pressure was kept constant during each test, while the pore pressure was varied in a special manner with a screw control connected to a mercury filled U-tube. The tests were performed with the constant  $-\sigma_1'$  curve hopping technique where the major principal stress jumps between the two preselected values  $\sigma_1'$  high and  $\sigma_1'$  low. The tests were started at the  $\sigma_1'$  high pressure level. After obtaining some data on this level, the pore pressure is increased to reach the  $\sigma_1'$  low level, and the deviator stress will decrease. After some time, usually within 20 minutes, the deviator stress levels off, some more

data are taken and the test is ready for the next jump, back to the  $\sigma_1'$  high curve, etc.

The internal drains of wool yarn and the external filter paper help ensure uniform pore pressure in the specimen. During the test, the pore pressure must be adjusted periodically to hold  $\sigma_1'$  at the desired constant value. The volume changes in the specimen during the test were found to be small, about 1% volume change during the complete test. The tests were carried to approximately 2-4% average vertical strain and apparent  $(\sigma_1 - \sigma_3)_{\max}$  and then stopped.

After test the sample was weighed, measured and the dry weight determined after the sample dried in a 105°C oven for two to three days.

Three additional IDS tests were performed in order to try the new hourglass shape of sample used in test series II. These tests were consolidated at 1 kg/cm<sup>2</sup>.

### Experimental results

The stresses in kg/cm<sup>2</sup> and strain in percent were computed on an electronic desk computer, the Olivetti Programma 101. The sample area is corrected for strain  $A = A_0 \frac{1}{1 + \epsilon_3}$ ,  $\epsilon_3 > 0$  where  $A_0$  is the area of sample after consolidation and before test, and  $\epsilon_3$  is the vertical strain. It was assumed that the stresses and strains were uniform throughout the sample. Volume changes during test were not taken into account in the area computation. The volume changes during test were about 1% of the total volume.

The stress-strain curves are drawn for  $\sigma_1'$  high and  $\sigma_1'$  low for each test. See Figures 17 and 18 for examples of stress-strain curves. Three to four values of  $\epsilon_3$  are selected and the deviator stressed is read from the graph. By inputting the values of  $\sigma_1'$  high,  $\sigma_1'$  low,  $(\sigma_1 - \sigma_3)$  high,  $(\sigma_1 - \sigma_3)$  low the I and D components,  $d = \frac{D}{\sigma_t}$  and  $\bar{\sigma}_t'$  are computed using the desk computer. For each test the maximum value of the I component is chosen. See Figures 14 to 20 and Table 3 for experimental results.

$I_{\max}$  was then graphed as a function of  $\sigma_t'$  (Figure 14). A straight line is fitted through the points, using a linear regression analysis, least squares. A 95% confidence interval is found for the extrapolated intercept  $I_0$ . Similar lines from previous compression test work by Schmertmann and current work by Ho are also shown for comparison. The results from this series are seen to be in good agreement with this previous work on extruded kaolinite.

It appears that some of the tests are stopped too early because the I component is still climbing at end of test. Particularly test nos. 305, 308, 310 and 314 were not carried far enough and therefore not included in the regression analysis. The maximum value of the I component seems to be adequately defined for the rest of the tests.

Test no. 319 was the first test on a tension sample. The stress-strain curve was not well defined, and this test was also taken out of the regression analysis.

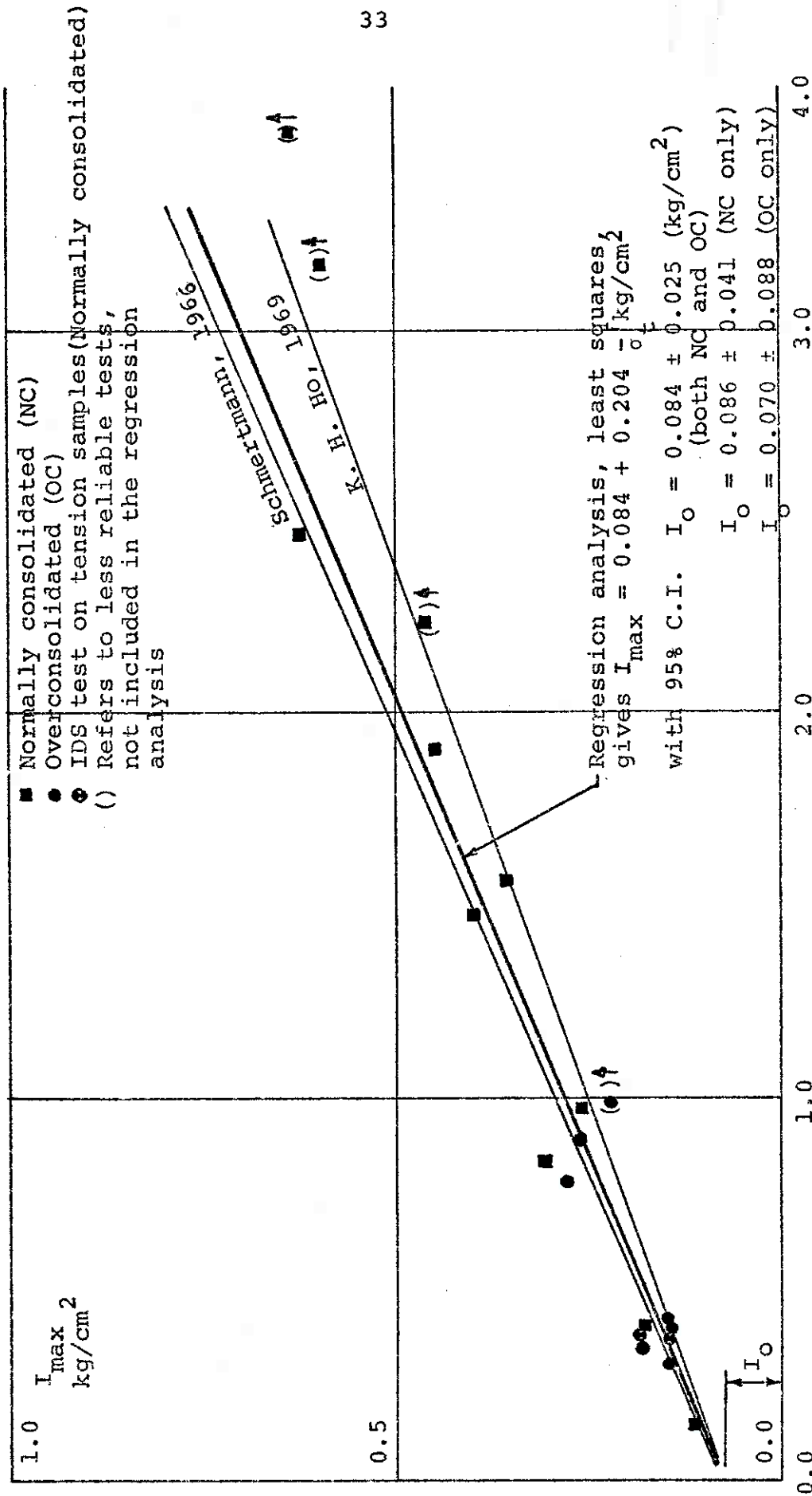


Figure 14. The I component as a function of the average effective stress,  $\sigma'_{at}$  at Mohr circle tangent point



In Professor Schmertmann's compression tests the I value reached its maximum at about 1/2 to 1% vertical strain and dropped as strain increased. He noticed that the I value reached its maximum for the high values of  $\sigma_1'$  at the low strain, and maximum is reached at a much larger strain when  $\sigma_1'$  is low. See Table 3 for strain at  $I_{\max}$  for the series I tests.

The tests were stopped before any necking of the sample could be observed. Diameter measurements of these samples after extension testing showed that the samples deform rather uniformly. Stress-dilatancy correction for the IDS test may not be needed because both curves have same corrections.

Figure 15 shows that overconsolidation does not increase the D component at strain of  $I_{\max}$  as was found by Schmertmann. However,  $I_{\max}$  in his compression tests occurred at less strain, about 1/2%. The stress-strain curves from an overconsolidated sample in this study do not differ noticeably from the stress-strain curves from a normally consolidated sample. A reason for this may be that in an extension test the samples are in a way all overconsolidated; the minor principal stress is decreasing.

#### Water content, degree of saturation and void ratio

The wet sample was weighed before and after each test, and finally weighed after oven drying. The sample diameter was measured at six positions and the height three positions before and after each test, with a vernier calipers and to a precision of  $\pm 0.1$  mm. The final measurements of diameter were only used as a check for the variation of strain and not in the calculation of final void ratios. Several values of

water content, saturation and void ratio were computed (see Table 4 and Figures 21 and 22).

The volume change during consolidation was computed on the basis of the volume change read on the burette during consolidation. It may be noted that some values in Table 4 show computed final saturation to be over the theoretical limit of 100%,  $S > 1$ , i.e. that something in the measurements is not quite correct. The writer then tried to compute final saturations using the volume change computed on the basis of the difference in the final and initial weights. This method did not give the same volume change and it did not give better values, so the first method was selected.

### Conclusions

From this test series the writer concludes:

1.  $I_{\max}$  as a function of the effective stress is the same in extension as in compression. The bond strength can be determined either way.
2. The value of the intermediate principal stress,  $\sigma_2 = \sigma_1$  in extension but  $\sigma_2 = \sigma_3$  in compression, does not significantly change  $I_{\max}$ .
3. The type of strain (tension or compression) makes no difference to  $I_{\max}$ , although it appears that I and D components mobilize at different strain.
4. Overconsolidation does not increase the I component in extension tests, as was also found by Schmertmann and by Ho in compression tests.
5. The bond strength with a 95% confidence interval is

$$I_0 = 0.084 \pm 0.025 \text{ (kg/cm}^2\text{)}$$

Table 3. Results from test series I

Test No.	$\sigma_{\text{cons}}$ kg/cm <sup>2</sup>	$t_{100}$ min	Back Pressure kg/cm <sup>2</sup>	Rate of Strain %/hour	$\sigma_1$ high kg/cm <sup>2</sup>	$\sigma_1$ low kg/cm <sup>2</sup>	$\epsilon_3$ %	$d = \frac{D}{\sigma_t}$	$I_{\text{max}}$ kg/cm <sup>2</sup>	D kg/cm <sup>2</sup>	$\sigma_t$ kg/cm <sup>2</sup>
301	2	46	3	0.49	1.86	1.46	2.8✓	0.329	0.303	0.288	0.828
302	3	120	2	0.49	2.85	2.25	2.4✓	0.275	0.394	0.420	1.469
303	4-2	75	2	0.49	1.90	1.50	2.4✓	0.333	0.259	0.314	0.889
304	6-1	68	2	0.34	0.95	0.75	1.6✓	0.324	0.149	0.149	0.433
305	6-2	40	2	0.34	1.90	1.50	1.2✓	0.294	0.218*	0.305	0.991
306	4-1	45	2	0.34	0.95	0.75	1.35✓	0.375	0.142	0.162	0.400
307	1	45	2	0.49	0.95	0.75	1.7✓	0.327	0.177	0.140	0.405
308	4	160	2	0.49	3.80	3.00	1.5✓	0.212	0.453*	0.485	2.236
309	0.5	60	2	0.49	0.48	0.38	1.6✓	0.401	0.114	0.067	0.154
310	6	55	2	0.49	5.70	4.50	1.5✓	0.191	0.628*	0.683	3.510
311	2	55	4	0.49	1.90	1.50	1.6✓	0.288	0.252	0.292	0.969
312	3	130	4	0.49	2.85	2.25	1.6✓	0.255	0.355	0.471	1.556
313	4	130	4	0.49	3.80	3.00	3.7	0.314	0.447	0.630	1.909
314	6	60	3	0.49	5.70	4.50	2.4✓	0.267	0.588*	0.879	3.171
315	5	80	2	0.49	4.75	3.75	3.9	0.279	0.622	0.716	2.468
316	6-2	85	3	0.49	1.90	1.50	3.7	0.391	0.276	0.332	0.781
317	6-1	70	3	0.49	0.95	0.75	3.6	0.379	0.183	0.147	0.358
318	4-1	55	3	0.49	0.95	0.75	3.0	0.482	0.144	0.173	0.314
319	1	--	2	0.89	0.95	0.75	1.6	0.413	0.225*	0.133	0.294
320	1	--	2	0.89	0.95	0.75	2.0	0.389	0.148	0.162	0.383
321	1	--	2	0.62	0.95	0.75	1.0	0.338	0.179	0.142	0.394

\* Indicates data not included in the regression analysis.  
 The results are simultaneous values for  $I_{\text{max}}$   
 Test nos. 319, 320 and 321 are IDS tests on tension samples

NC  
ext.

cc

Tens

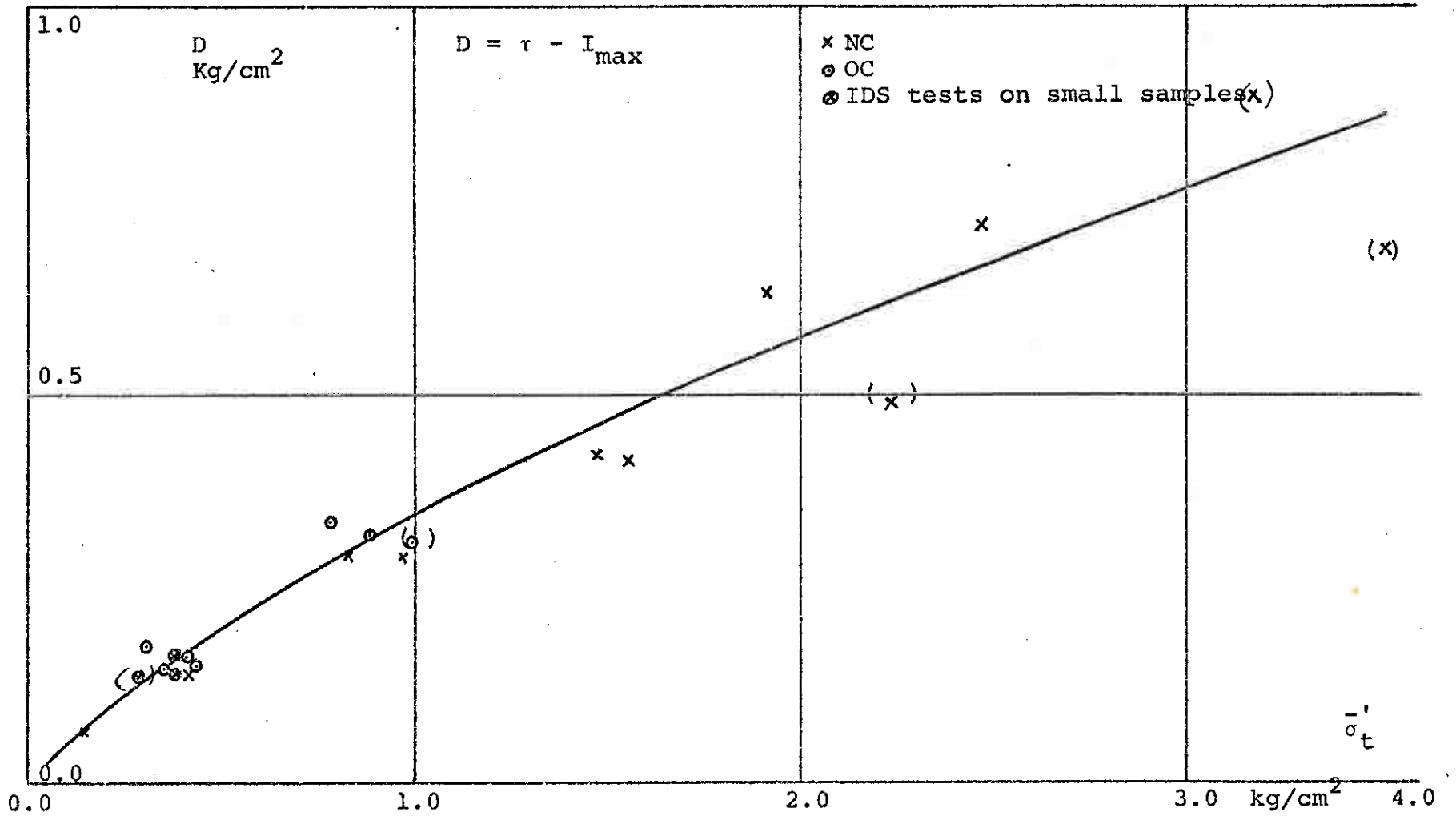


Figure 15. The D component at  $I_{\max}$  as a function of average effective stress

IDS Tests

- \*-x Normally consolidated
- Overconsolidated
- ⊙-⊙ IDS tests on tension samples
- For comparison
- ▲ Test series II
- Test series III without stress-dilatancy correction
- Test series II with stress-dilatancy correction

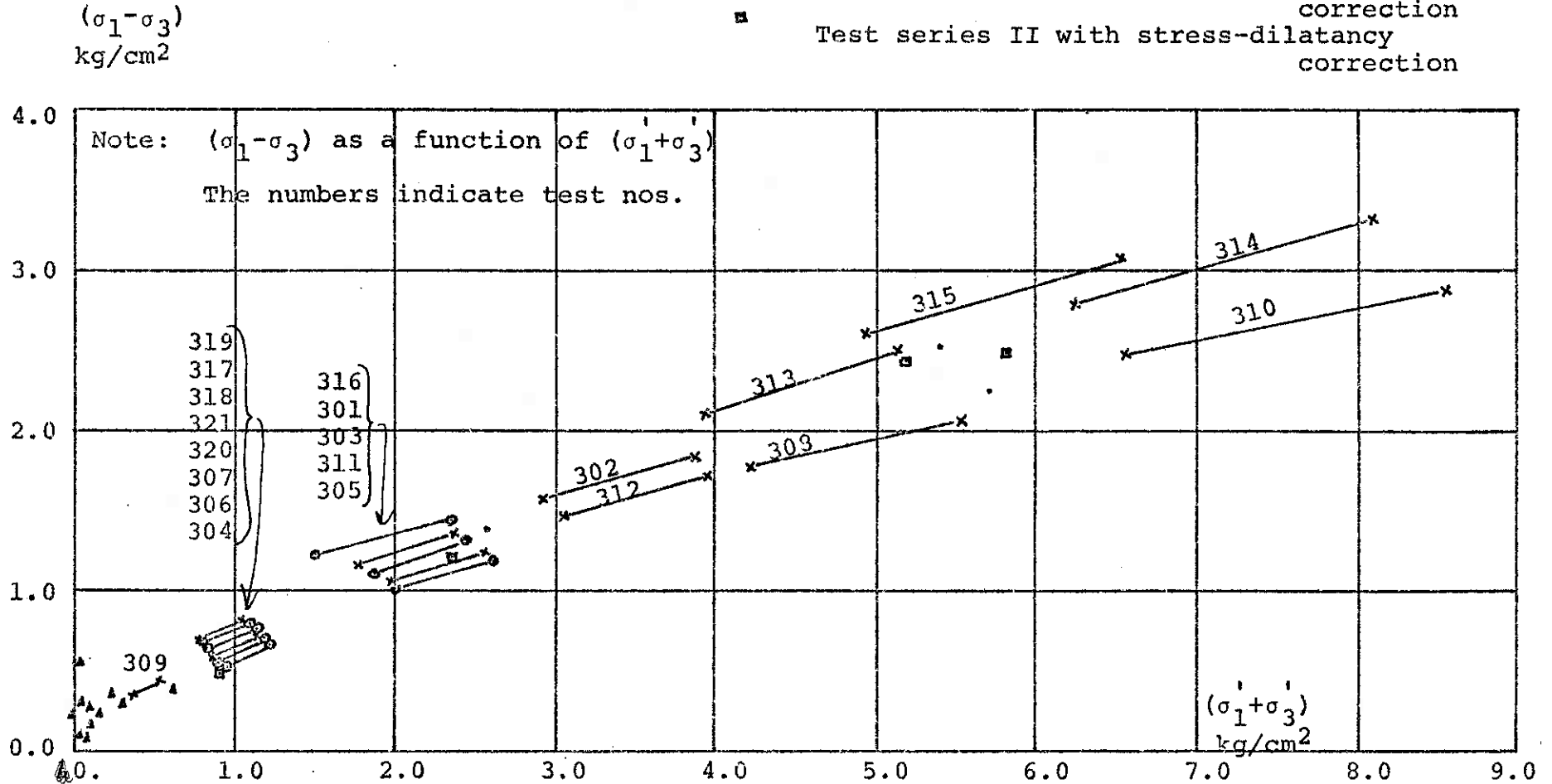


Figure 16. Series I - pieces of constant-structure envelopes at  $I_{max}$ . Series II and III -  $(\sigma_1 - \sigma_3)_{max}$  points of Mohr circles

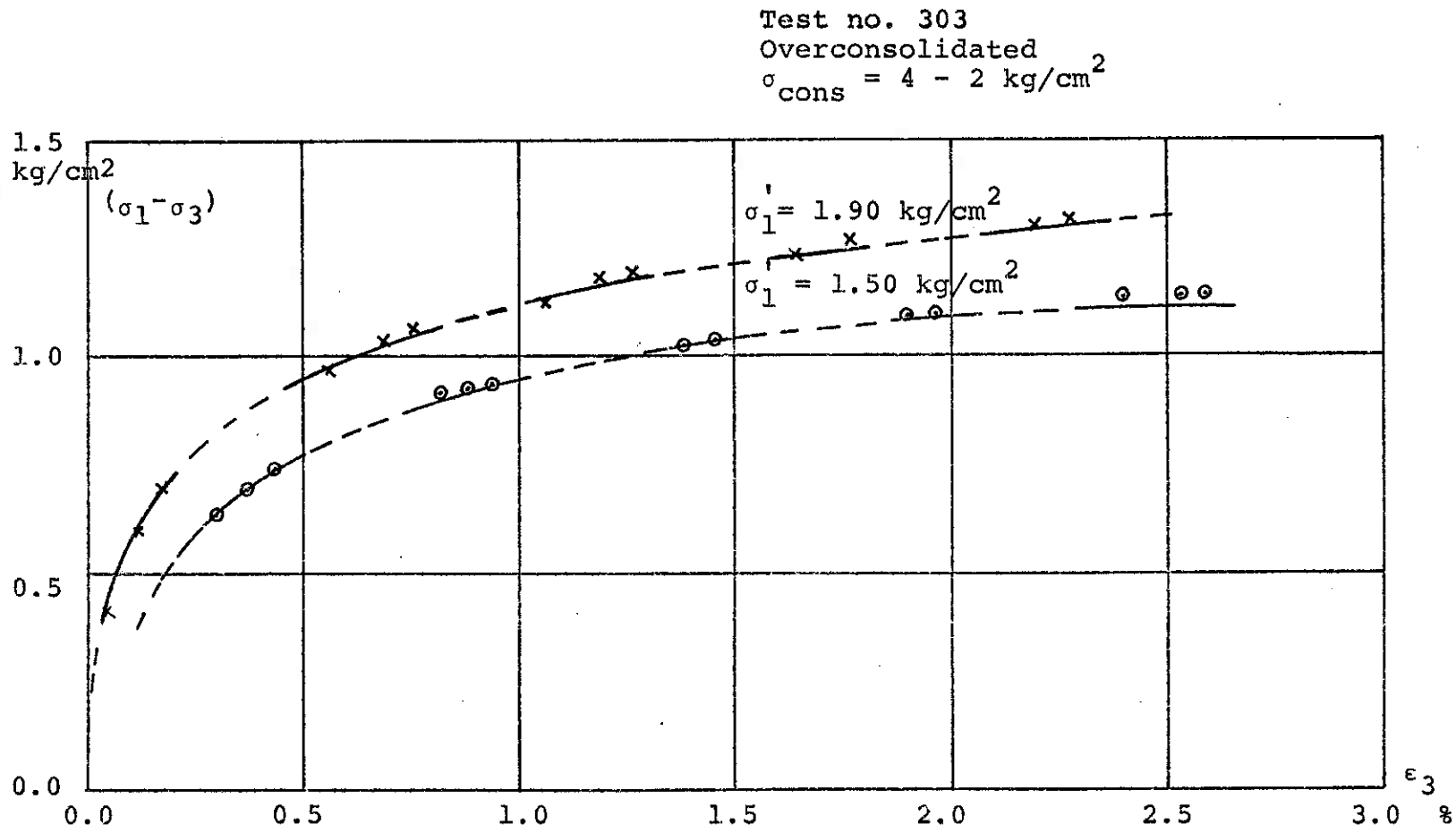


Figure 17. Example of stress-strain curve from IDS tests, overconsolidated specimen

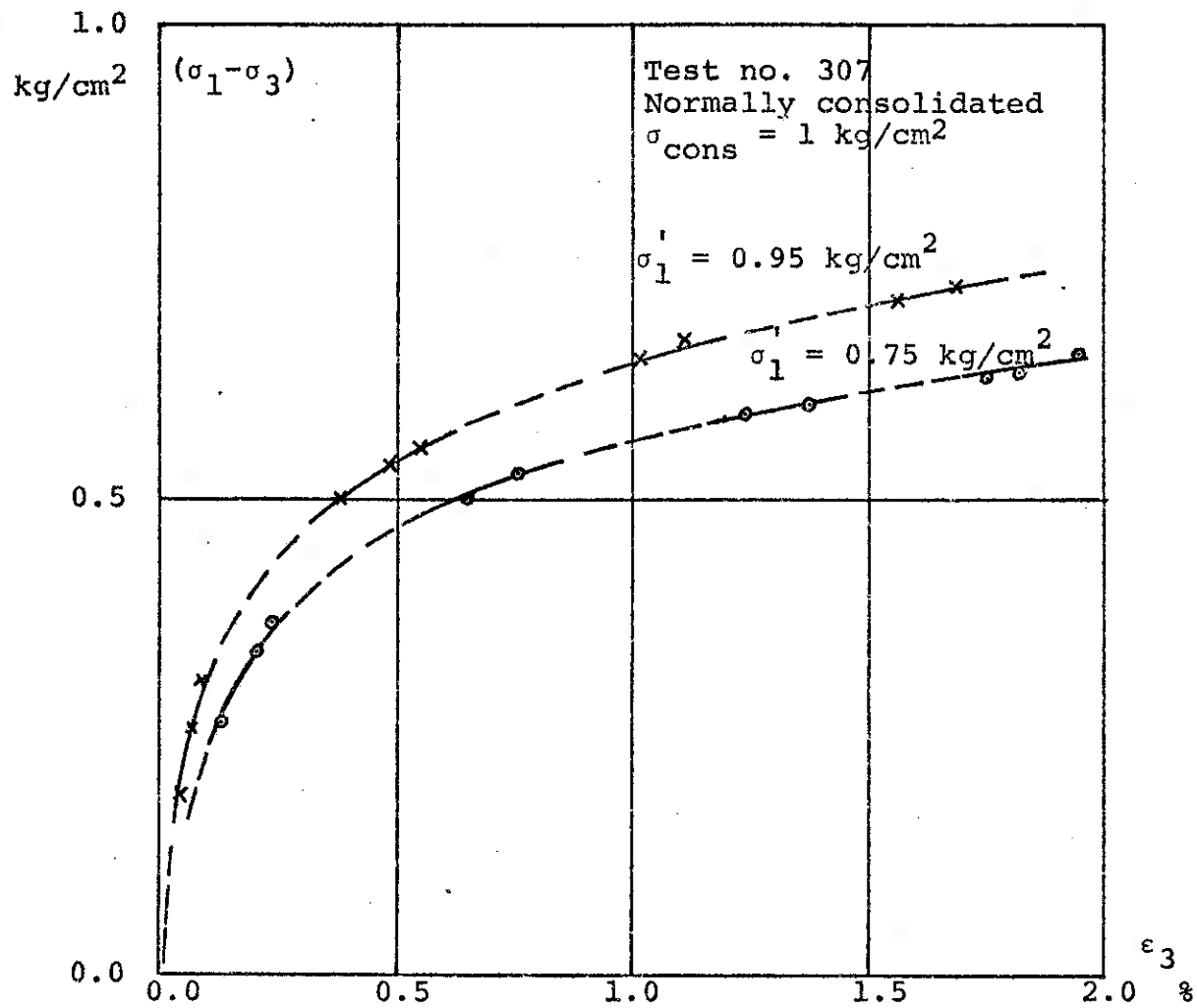


Figure 18. Example of stress-strain curve from IDS tests, normally consolidated specimen

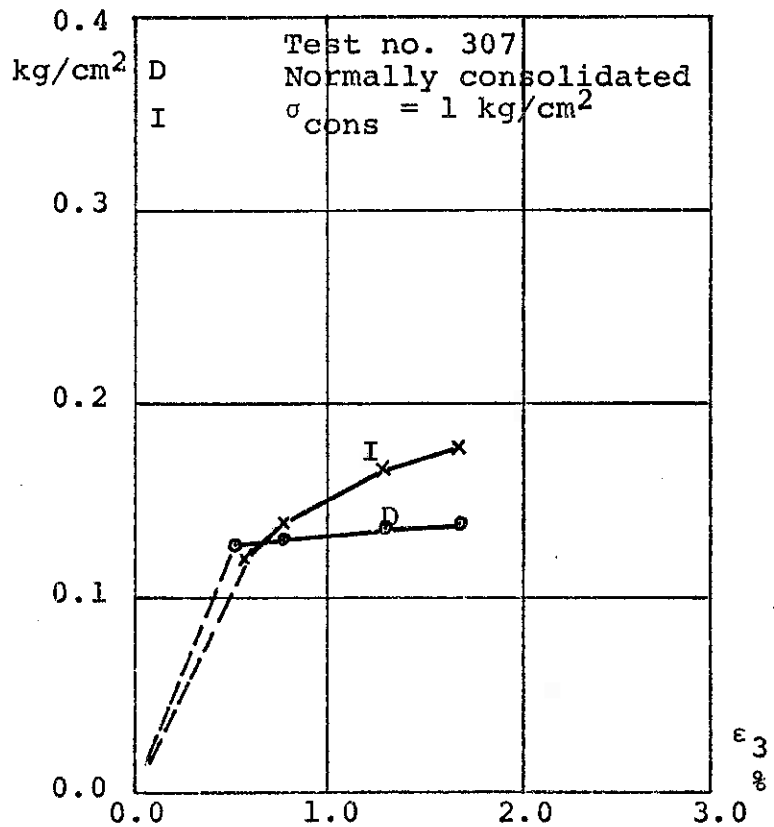


Figure 19. Example of the I and D component as a function of vertical strain for a normally consolidated specimen

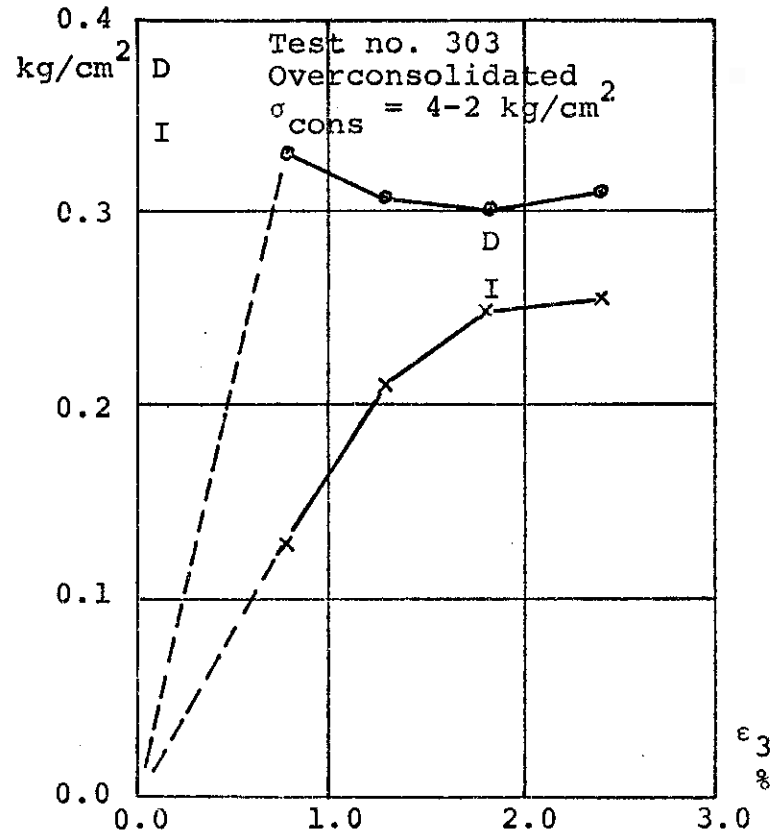


Figure 20. Example of the I and D component as a function of vertical strain for an overconsolidated specimen



Table 4. Water contents, degrees of saturation and void ratios from test series I samples

Test No.	Sample No.	$\sigma_{cons}$ Kg/cm <sup>2</sup>	$\frac{\sigma'}{\sigma_t}$ Kg/cm <sup>2</sup>	Before test			After conso. phase			After test		
				w <sub>i</sub>	S <sub>i</sub>	e <sub>i</sub>	w <sub>cons</sub>	S <sub>cons</sub>	e <sub>cons</sub>	w <sub>f</sub>	S <sub>f</sub>	e <sub>f</sub>
301	30	2	0.828	0.363	0.974	0.973	0.352	1.001	0.918	0.361	1.001	0.940
302	27	3	1.469	0.362	0.985	0.959	0.364	1.074	0.884	0.370	1.072	0.901
303	28	4-2	0.889	0.362	0.975	0.968	0.340	0.976	0.909	0.350	0.977	0.936
304	24	6-1	0.433	0.367	0.993	0.964	0.346	1.025	0.881	0.351	1.025	0.894
305	22	6-2	0.991	0.368	0.984	0.974	0.343	0.998	0.896	0.348	0.998	0.910
306	20	4-1	0.400	0.364	0.990	0.960	0.350	1.016	0.900	0.358	1.029	0.907
307	18	1	0.405	0.370	0.987	0.976	0.361	0.990	0.952	0.366	1.047	0.911
308	16	4	2.236	0.370	1.005	0.961	0.351	1.058	0.864	0.356	1.060	0.877
309	15	0.5	0.154	0.374	1.008	0.969	0.375	1.023	0.956	0.379	1.023	0.966
310	13	6	3.510	0.369	1.003	0.961	0.327	1.006	0.847	0.329	1.007	0.851
311	11	2	0.969	0.365	0.989	0.964	0.358	1.020	0.915	0.360	1.019	0.922
312	10	3	1.556	0.371	0.993	0.974	0.348	1.032	0.881	0.353	1.032	0.893
313	8	4	1.909	0.360	0.990	0.950	0.340	1.022	0.868	0.345	1.021	0.882
314	6	6	3.171	0.374	1.007	0.969	0.329	1.060	0.810	0.331	1.060	0.814
315	5	5	2.468	0.344	0.970	0.926	0.310	1.005	0.804	0.314	1.004	0.815
316	3	6-2	0.781	0.373	0.996	0.977	0.331	1.017	0.850	0.343	1.017	0.881
317	17	6-1	0.358	0.370	0.999	0.966	0.339	1.002	0.881	0.353	1.002	0.919
318	26	4-1	0.314	0.367	0.995	0.962	0.347	1.006	0.899	0.359	1.006	0.930
319	15a	1	0.294	---	---	---	0.373	---	---	0.375	---	---
320	18a	1	0.383	0.386	0.994	1.013	0.373	0.994	0.979	0.377	0.994	0.989
321	20a	1	0.394	0.385	0.985	1.019	0.371	0.985	0.982	0.374	0.985	0.990

\* Normally consolidated

⊙ Overconsolidated with numbers indicating the initial and rebound consolidation pressures in  $\text{kg}/\text{cm}^2$

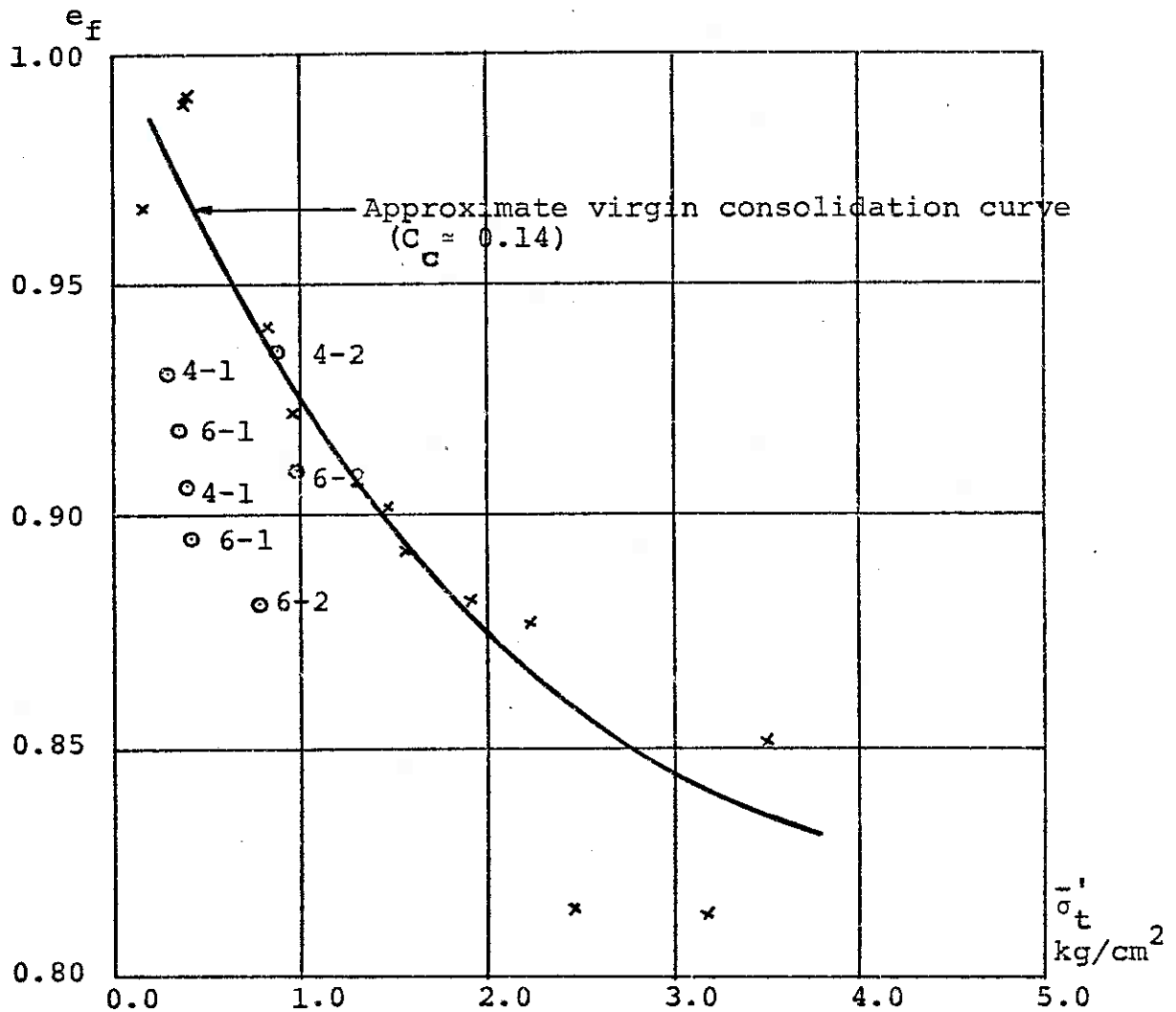


Figure 21. The final void ratio

- \* Normally consolidated
- o Overconsolidated with numbers indicating consolidation pressures

For comparison

- ▲ Test series II
- Test series III

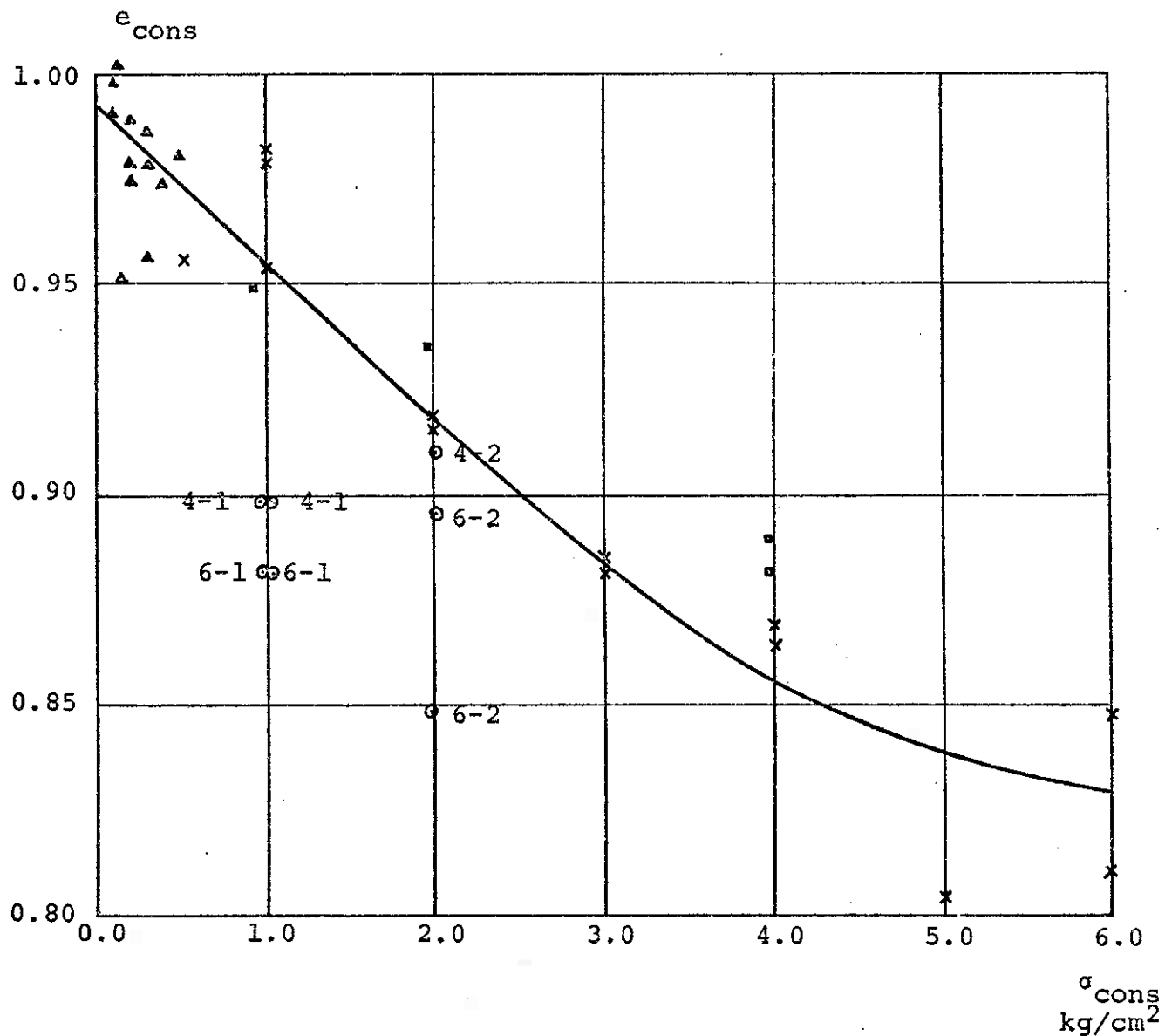


Figure 22. The void ratio after consolidation

## CHAPTER 5

### SERIES II - TESTS ON TENSION SAMPLES

#### Introduction

Bishop and Garga's very recent series of tension tests on London clay (18) inspired this series. This test technique makes it possible to extend the effective stress into negative values to obtain a negative minor effective stress. A sample with a reduced middle section permits this. The purpose is to find the bond strength, i.e. the shear resistance at zero effective stress (after eliminating any stress-dilatancy contribution).

#### Previous work

Bishop and Garga performed a series of tests on intact samples of blue, fissured London clay, using samples with reduced center sections and slow drained tests. Their test series showed that clay could withstand a tensile strength and that it was almost independent of  $\sigma_1'$  in the range examined, 0.21 - 0.70 kg/cm<sup>2</sup>. The tensile strength at failure was in the range of 0.27 - 0.34 kg/cm<sup>2</sup>, the tensile strength defined as

$$\sigma_3' = \sigma_1' - (\sigma_1 - \sigma_3)_{\max} \quad [12]$$

Bishop performed another test series in compression on the same clay remolded. He found the cohesion intercept very small, and concluded that remolding completely destroyed the bonding in the sample.

It should be noted that Bishop reports no stress-dilatancy corrections.

### Theoretical tension limit

The sample will detach from the end caps when the effective stress at the ends of the sample is zero or less than zero. When the axial effective stresses at the enlarged ends are zero, the axial effective stress at the middle of the sample will be negative. The following notation is used:

$\sigma'_E$  average axial effective stress on the ends of the sample

$\sigma'_C$  axial effective stress on the middle section

$A_E$  area of the end section

$A_C$  area of the middle section

$T$  tensile force

The axial effective stress on the ends of the sample is

$$\sigma'_E = \sigma'_1 - \frac{T}{A_E}, \text{ or } \sigma'_E = 0 \text{ when } T = \sigma'_1 A_E \quad [13]$$

and on the middle of the sample

$$\sigma'_C = \sigma'_1 - \frac{T}{A_C} \quad [14]$$

The limits for  $T$  are

$$\sigma'_C = \sigma'_1 - \frac{\sigma'_1 A_E}{A_C} \quad [15]$$

$$\sigma'_C = -\sigma'_1 \left( \frac{A_E}{A_C} - 1 \right) \quad [16]$$

Note

$$\sigma'_3 = \sigma'_C \quad [17]$$

For the extension test  $\sigma'_3$  will decrease until  $(\sigma'_1 - \sigma'_3)_{\max}$  is reached or until  $\sigma'_3 = -\sigma'_1 \left( \frac{A_E}{A_C} - 1 \right)$  is reached. Due to the rubber membranes  $\sigma'_3$  can exceed  $\sigma'_3 = -\sigma'_1 \left( \frac{A_E}{A_C} - 1 \right)$  slightly.

For this series of tests the area of the end section was  $A_E = 9.95 \text{ cm}^2$  and the area of middle section was  $A_C = 5.64 \text{ cm}^2$ , for a ratio of 1.76 resulting in the limiting negative value of  $\sigma'_3 = -0.76 \sigma'_1$ . Failure occurred before the limiting value of  $\sigma'_3$  was reached, except for test no. 333 where  $\sigma'_3$  was computed to be  $-1.02 \sigma'_1$ . Perhaps the membrane held this sample requiring a force in membrane of about 0.20 kg. Note also that  $A_C$  is decreasing during test, which will increase the limiting value of  $-0.76 \sigma'_1$ .

#### Set up of tension samples

The wax and wax paper covering was removed from the soil sample. Only one axial internal wool drain was inserted in the sample. Using a template the sample is trimmed with wire saw and straight edge to a diameter of 2.68 cm in the reduced section. Figures 23 and 24 show the dimensions of specimen and trimming of the samples. Trimming took about six minutes.

The sample was cut to a height of 8 cm and placed on the pedestal. Because of the problem of trapped air between

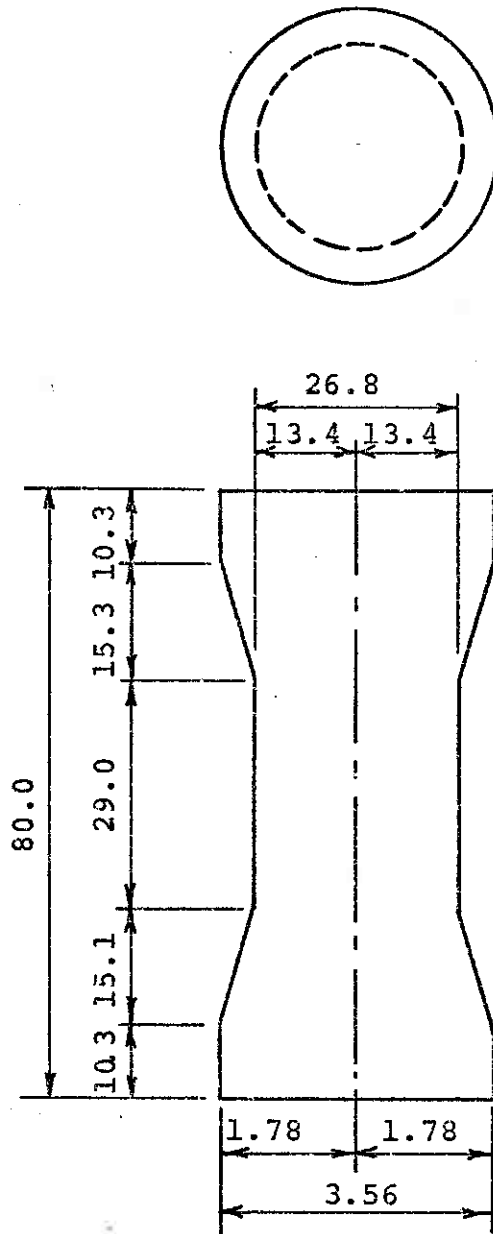
membranes, a single membrane was used rather than the usual two. A very low vacuum was used to remove the air trapped between rubber membrane and sample. Silicone grease was applied over the membrane. To reinforce the sample as little as possible, no external filter strips were used. The drainage was through one internal drain to the bottom filter stone only.

### Consolidation

Because of the low cell pressures at which this series of tests was performed, the volume increased instead of decreased during the consolidation phase. This means that these samples at these pressures could be considered as overconsolidated by the pressures of the "Vac-Aire" extrusion. The consolidation cell pressure was maintained overnight and the test run the next day. During consolidation there were air bubbles escaping into the burette. This was probably due to the air trapped between the clay and the vertical folds of the surrounding membrane. The specimens were all consolidated hydrostatically. To compensate for the uplift, weights were placed directly on the piston.

### The tension tests

The tests were run as drained tests at a constant rate of total sample elongation. No back pressure was used and the cell pressure was kept constant. The drainage tube from the sample was connected to a bowl of water with its surface



Scale 1:1  
Dimensions in mm

Figure 23. Sketch of tension specimen with dimensions



at the same height as the middle of the sample. Figure 25 shows a photograph of this test. During the test, the deviator stress, vertical strain and volume change of sample were recorded and plotted. In every case the volume of the sample increased during the test.

The time for primary consolidation,  $t_{100}$ , could not be obtained from the consolidation phase because the volume change was too small for an accurate time curve to be measured. Different trial rates of strain were used for the tests, but the rate of strain did not seem to affect the shear strength. The writer believes the goal of zero pore pressure during strain was essentially achieved in all tests.

The test was stopped when the maximum value of  $(\sigma_1 - \sigma_3)$  was reached. The  $(\sigma_1 - \sigma_3)_{\max}$  was reached before the development of observable failure planes.

#### Experimental results

After some experimentation, described later, it was assumed that the vertical strain develops uniformly over the entire middle section and half of the transition sections, i.e. over a height of 4.42 cm (see Figure 23).

The area of sample was computed according to the formula  $A = A_0 \frac{1}{1 + \epsilon_3}$ ,  $\epsilon_3 > 0$ . Volume changes during test were not taken into account in the area computation. The volume changes during the test were negligible, only about 0.4% of the total volume at failure. The stresses and strains were computed, using the desk computer. See Figure 32 for an example stress-strain curve.

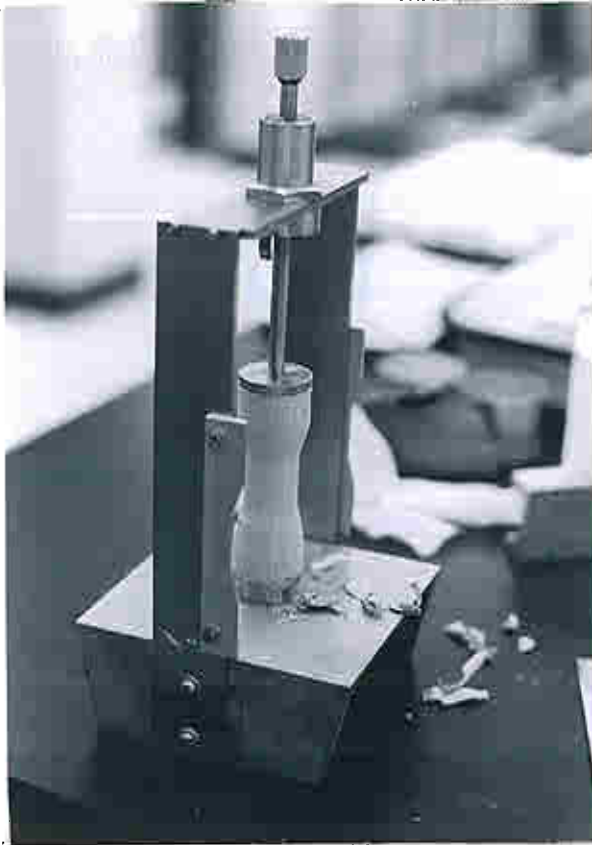


Figure 24.  
Trimming of tension  
sample with reduced  
middle section

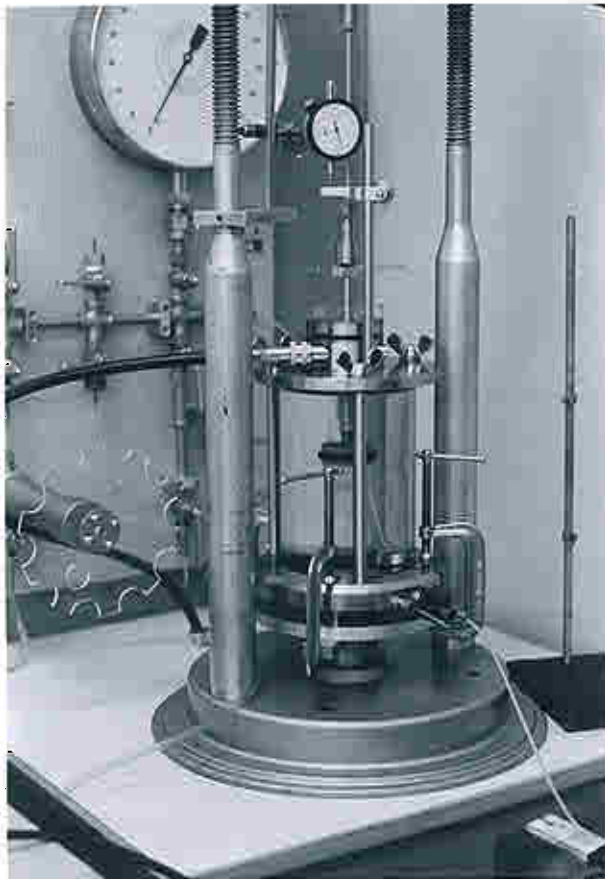


Figure 25.  
Performance of test  
in test series II



Figure 26. Sample with failure planes and heads of straight pins

To find the cohesion of the soil, first plot the top points of all the Mohr circles at failure. For convenience the writer used coordinates  $(\sigma_1 - \sigma_3)_{\max}$  and  $(\sigma_1' + \sigma_3')$ . Ideally these points would lie on a straight line intercepting with  $(\sigma_1 - \sigma_3)$  axis. Dividing the intercept by  $2 \cos \phi$  yields the  $\sigma' = 0$  shear strength. See Figure 27. However, the reader will see a large scatter in the data points intended to define the line. The best line, least squares, was fitted through the points and a  $\sigma' = 0$  shear strength of  $0.112 \text{ kg/cm}^2$  was obtained, with a 95% confidence interval of  $\pm 0.041$ .

Test no. 331 is not included in the analysis because the results differ so much from the other data and it was noticed during trimming that the specimen was much harder than the other specimens. In Figure 28  $(\sigma_1 - \sigma_3)_{\max}$  is plotted as a function of the final void ratio. It is seen that there is a definite relationship between void ratio and the failure strength. Table 5 gives a summary of the test conditions and results.

Because the above  $\sigma' = 0$  strength includes a contribution due to the soil expanding against the cell pressure, this strength is somewhat greater than bond strength only. The tests were therefore recomputed with stress-dilatancy correction. See the next chapter for a description of the stress-dilatancy theory. The accuracy of such correction in this test series is uncertain because the distribution of strain and volume change was only known approximately.

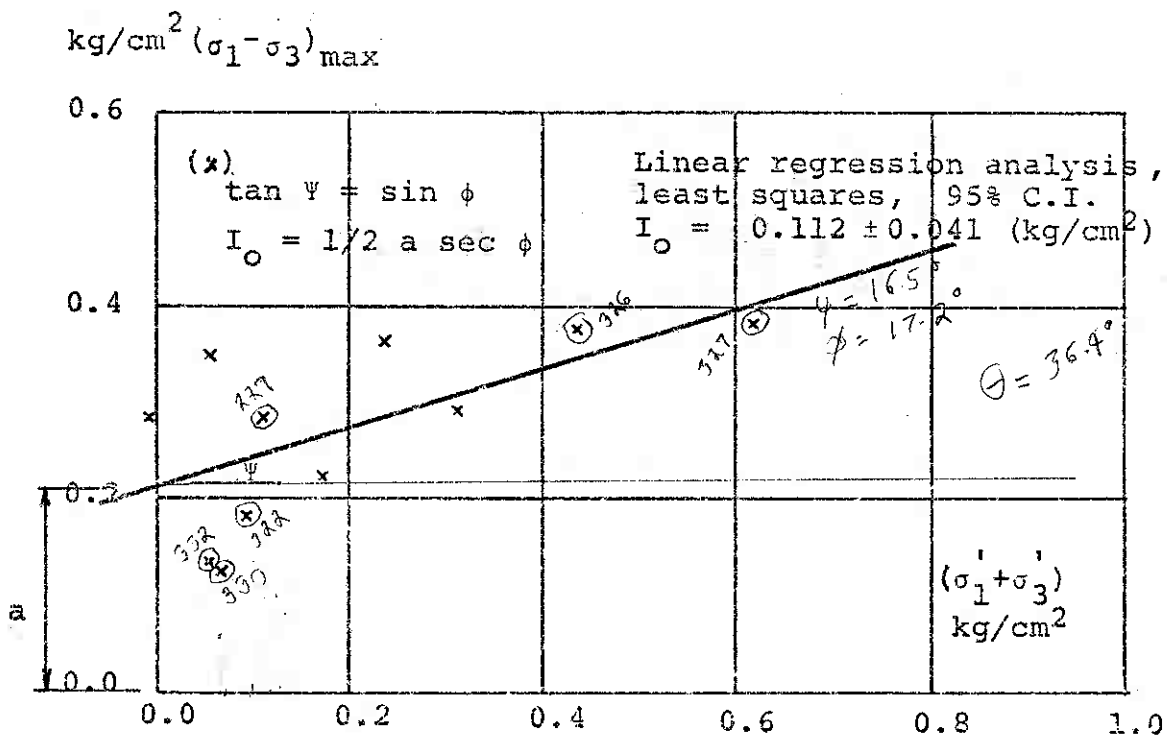


Figure 27. ( $\sigma_1 - \sigma_3$ )<sub>max</sub> as a function of ( $\sigma_1 + \sigma_3$ ) before stress-dilatancy correction

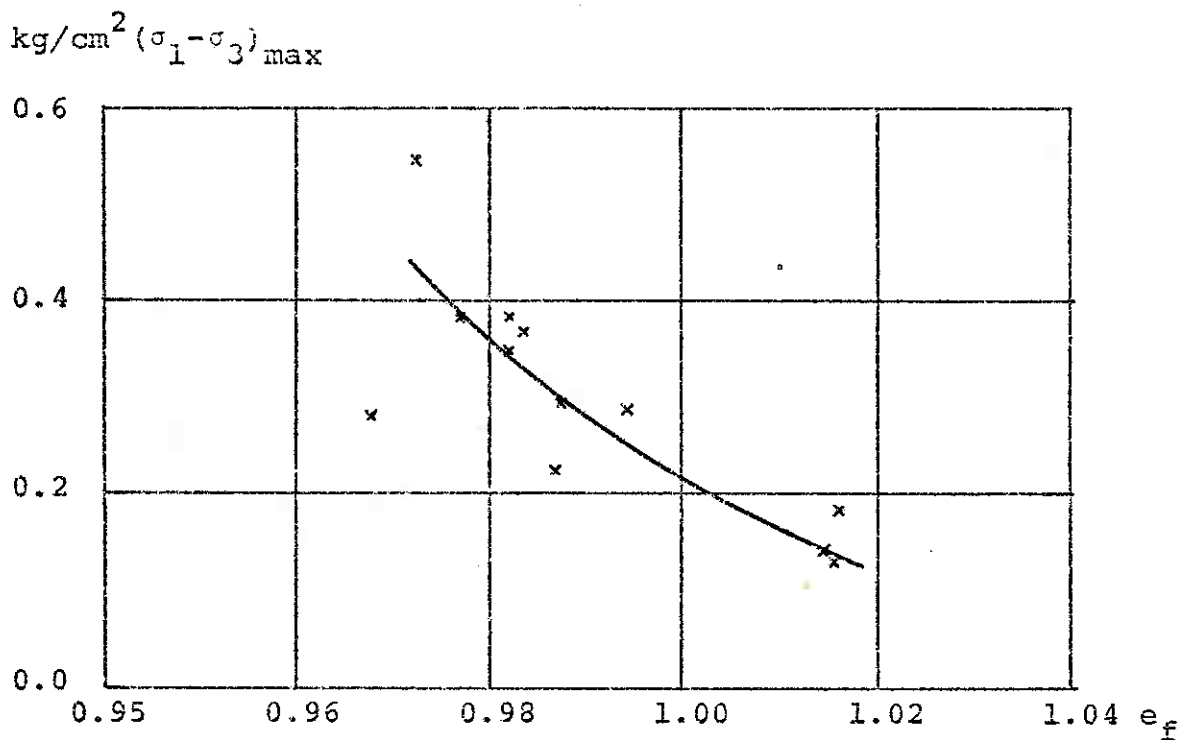


Figure 28. ( $\sigma_1 - \sigma_3$ )<sub>max</sub> as a function of the void ratio at end of test for entire sample

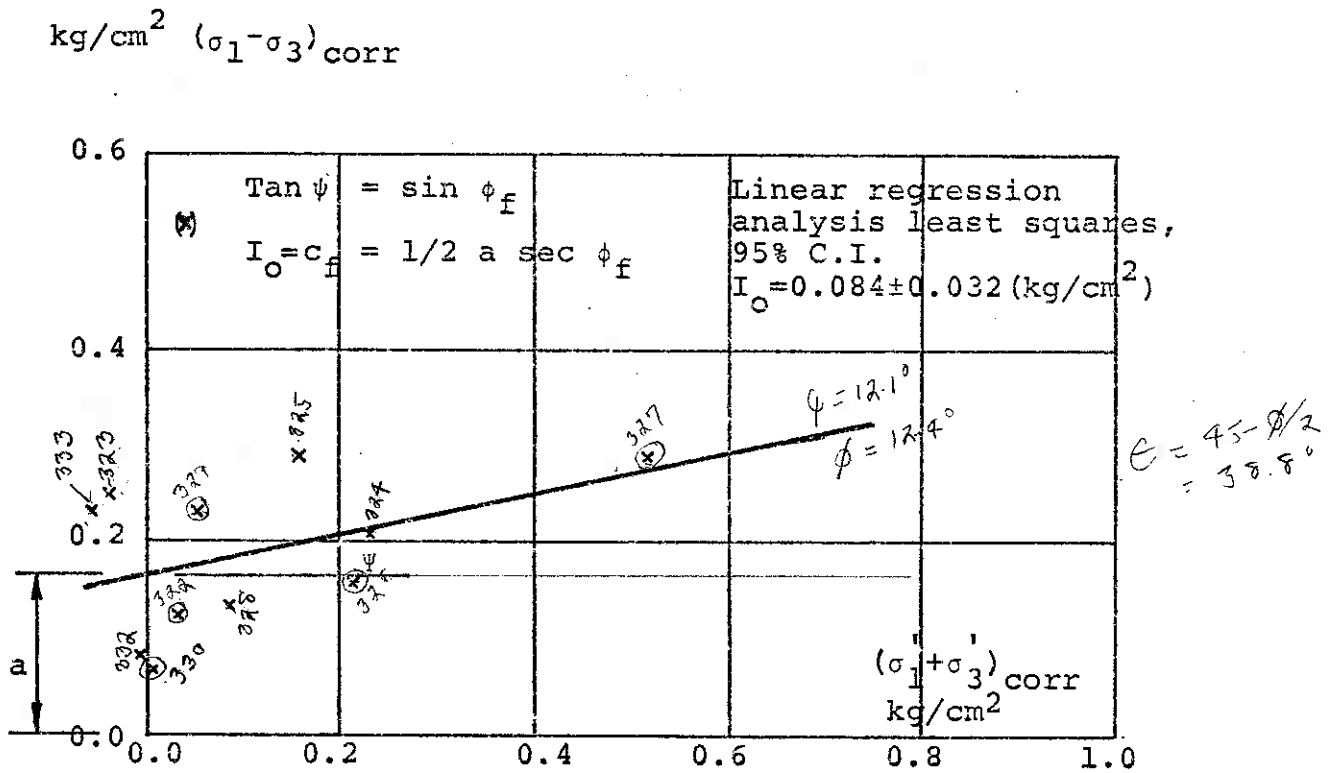


Table 5. Results from test series II

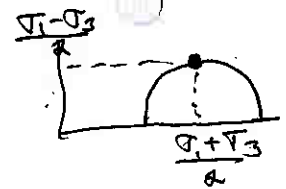
Test No.	Strain Rate %/hour	$\epsilon_3$ at Failure %	$\sigma_1$ kg/cm <sup>2</sup>	$(\sigma_1 - \sigma_3)_{\max}$ kg/cm <sup>2</sup>	$(\sigma_1 + \sigma_3)$ kg/cm <sup>2</sup>	With Stress-Dilatancy Correction	
						$(\sigma_1 - \sigma_3)_{\text{corr}}$ kg/cm <sup>2</sup>	$(\sigma_1 + \sigma_3)_{\text{corr}}$ kg/cm <sup>2</sup>
322	0.89	1.47 <i>1.65</i>	0.141	0.185	0.096	0.123	0.033 ✓
323	0.62	2.42 <i>3.9</i>	0.204	0.348	0.059	0.249	-0.040 ✓
324	0.62	1.02 <i>1.65</i>	0.301	0.291	0.310	0.210	0.230 ✓
325	0.62	0.68 <i>0.91</i>	0.301	0.366	0.236	0.289	0.159 ✓
326	0.09	0.41 <i>4.56</i>	0.406	0.375	0.436	0.158	0.218 ✓
327	0.09	0.49 <i>5.99</i>	0.498	0.382	0.613	0.287	0.517 ✓
328	0.62	0.77 <i>1.24</i>	0.199	0.221	0.176	0.132	0.087 ✓
329	0.31	1.22 <i>3.94</i>	0.199	0.287	0.110	0.229	0.051 ✓
330	0.09	1.84 <i>10.4</i>	0.097	0.129	0.064	0.067	0.002 ✓
331*	0.62	3.28	0.299	0.543	0.054	0.524	0.035
332	0.62	0.68 <i>1.10</i>	0.097	0.137	0.056	0.079	-0.0016 ✓
333	0.62	1.58 <i>4.55</i>	0.139	0.281	-0.003	0.229	-0.054 ✓

*E = 0.55 kg/cm<sup>2</sup>*  
*T = 0.28*  
*E = 1.14*  
*T = 0.630*

\* Indicates test not included in the regression analysis.

Table 5. Results from test series II

for Mike A  
11 pts, ÷ by 2



With Stress--Dilantancy Correction

Test No.	Strain Rate %/hour	$\epsilon_3$ at Failure %	$\sigma_1$ kg/cm <sup>2</sup>	$(\sigma_1 - \sigma_3)_{max}$ kg/cm <sup>2</sup>	$(\sigma_1 + \sigma_3)$ Kg/cm <sup>2</sup>	$(\sigma_1 - \sigma_3)_{corr}$ kg/cm <sup>2</sup>	$(\sigma_1 + \sigma_3)_{corr}$ kg/cm <sup>2</sup>
322	0.89	1.47	0.141	0.185	0.096	0.123	0.033
323	0.62	2.42	0.204	0.348	0.059	0.249	-0.040
324	0.62	1.02	0.301	0.291	0.310	0.210	0.230
325	0.62	0.68	0.301	0.366	0.236	0.289	0.159
326	0.09	0.41	0.406	0.375	0.436	0.158	0.218
327	0.09	0.49	0.498	0.382	0.613	0.287	0.517
328	0.62	0.77	0.199	0.221	0.176	0.132	0.087
329	0.31	1.22	0.199	0.287	0.110	0.229	0.051
330	0.09	1.84	0.097	0.129	0.064	0.067	0.002
<del>331*</del>	<del>0.62</del>	<del>3.28</del>	<del>0.299</del>	<del>0.543</del>	<del>0.054</del>	<del>0.524</del>	<del>0.035</del>
332	0.62	0.68	0.097	0.137	0.056	0.079	-0.0016
333	0.62	1.58	0.139	0.281	-0.003	0.229	-0.054

$E = 0.977 \times 10^4$   
 $\nu = 0.28$   
 $E = 1.14$   
 $\nu = 0.630$

\* Indicates test not included in the regression analysis.



Assuming that the height change and volume change occurred only over the entire middle section and half of the transition sections, the computation with the stress-dilatancy correction gives the following bond strength with the 95% confidence interval  $I_0 = 0.084 \pm 0.032$  (kg/cm<sup>2</sup>). See Figure 29.

As more tests were performed, the results were not as consistent with previous tests as expected. Because of this unexpected scatter the load cell was calibrated again, and the mercury pot constant pressure system was recalibrated. Both  $(\sigma_1 - \sigma_3)$  and  $\sigma_h$  proved accurate.

The pore pressure was not checked, and time for primary consolidation,  $t_{100}$ , was not obtained. The kaolinite has a relatively high permeability and the writer assumed that the pore pressure could be assumed zero with negligible error. Supporting this assumption is the fact that these tests, which used an internal wool drain to assist pore pressure dissipation, were performed over several hours, averaging 5 1/2 hours, and that  $(\sigma_1 - \sigma_3)_{\max}$  was not affected by the rate of strain.

The writer believes the scatter in the results is due to variations in specimen void ratios.

#### Water content, degree of saturation and void ratio

The water content, degree of saturation and void ratio were determined for the condition after trimming but before consolidation, after consolidation and the final after-test values. See Table 6.

Due to the hourglass shape of these specimens their volumes were difficult to obtain by measuring. To get an approximate

volume the diameter and height were first determined for the untrimmed 3.58 X 10 cm sample. The volume of the trimmed sample was then set equal to the volume of the big sample multiplied by the ratio of their initial weights.

Due to the small volume change and the air bubbles during consolidation the volume change could not be read accurately on the burette. The total volume change was set equal to the difference in the after-test and before-test weight of trimmed sample.

#### Distribution of strain

Heads of straight pins were inserted along the sides of three samples, as illustrated in Figure 26. The distance to the heads was measured with a vernier calipers before and after the test, and a rough determination of the distribution of vertical strain was obtained, see Figure 30.

It is seen that the middle, reduced section, has most of the strain, especially where the section includes the failure planes. The transition sections have some and the end sections have almost none, or even negative, tensile strain. When the sample is taken down there is some unknown distribution of strain rebound, so this pin method is not a very exact measurement of the distribution of strain. Only a few tests were carried far enough that failure planes and necking developed because  $(\sigma_1 - \sigma_3)_{\max}$  is reached first. The mode of failure planes and necking is seen in Figure 26, and compares well with the theoretical predictions illustrated in Figure 2.

### Distribution of water content

For some samples the initial water content was determined from the end cut and center cut trimmings from the sample. The water content determined from these thin trimmings was less than the overall initial water content. The error is due to drying, although much care was taken to weight the trimmings as quickly as possible. It appears that such testing must be done in a humid room which was not available for this study.

After the test, some of the samples were cut into horizontal slices and the water content determined. Figure 31 shows the distribution of water content. It is seen that the middle parts of tests 330 and 332 have more volume increase than the rest of the specimen, while for tests 328 and 329 the volume increase is more uniform.

### Conclusions

From this tension test series with drained test performed on hourglass shaped samples in the low range of effective stresses  $0.0 - 0.3 \text{ kg/cm}^2$  on the plane of failure at failure, the writer concludes that:

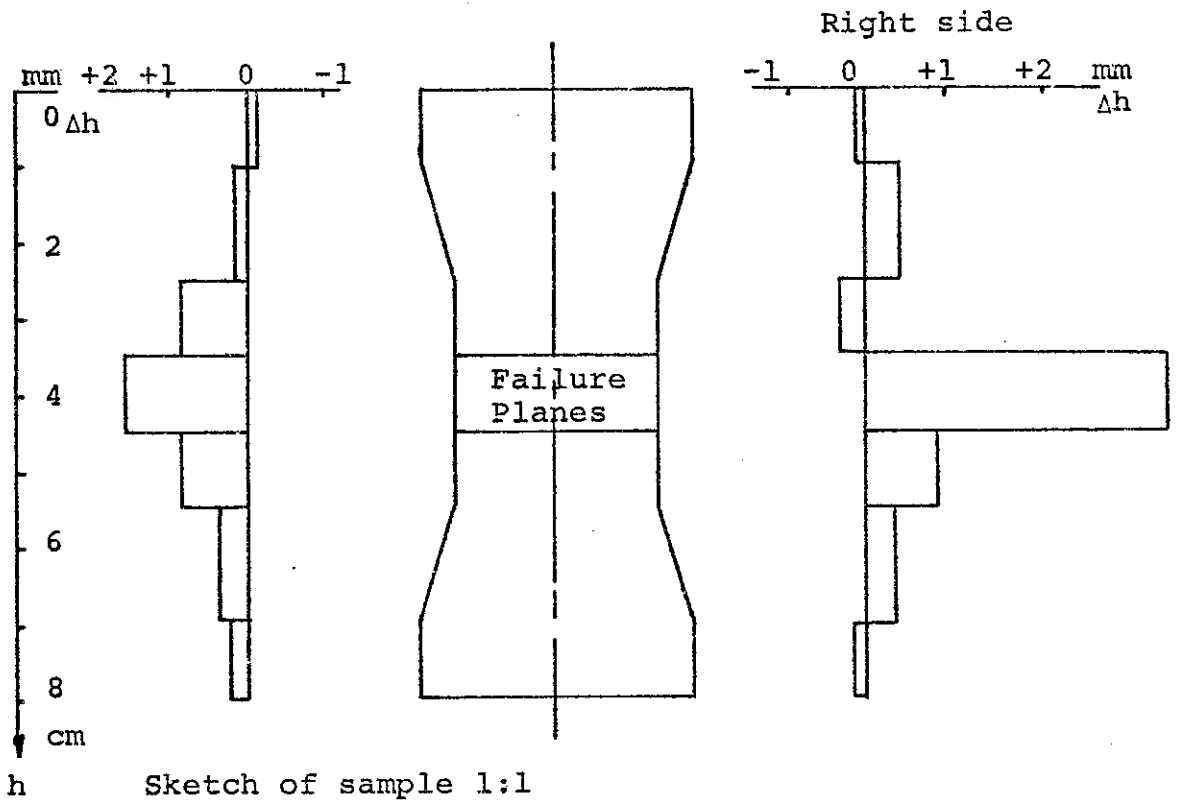
1. The shear strength is dependent on the effective stress and the void ratio of specimen.
2. The extruded kaolinite has a bond strength.
3. The "bond strength" without stress-dilatancy correction, with a 95% confidence interval, is:

$$I_0 = 0.112 \pm 0.041 \text{ kg/cm}^2$$

4. The bond strength after approximate stress-dilatancy correction, with a 95% confidence interval, is:

$$I_0 = 0.084 \pm 0.032 \text{ (kg/cm}^2\text{)}.$$

61  
Test no. 331



Test no. 333

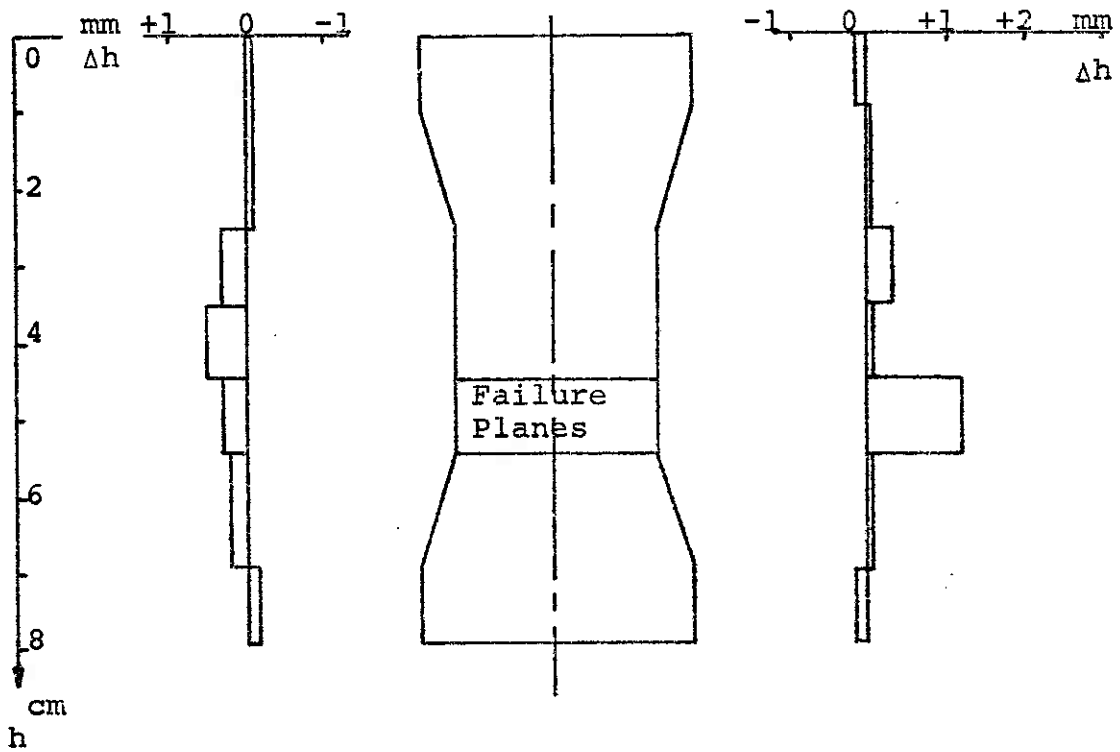


Figure 30. Distribution of vertical strain after test by measuring pin spacings on opposite sides of sample after test

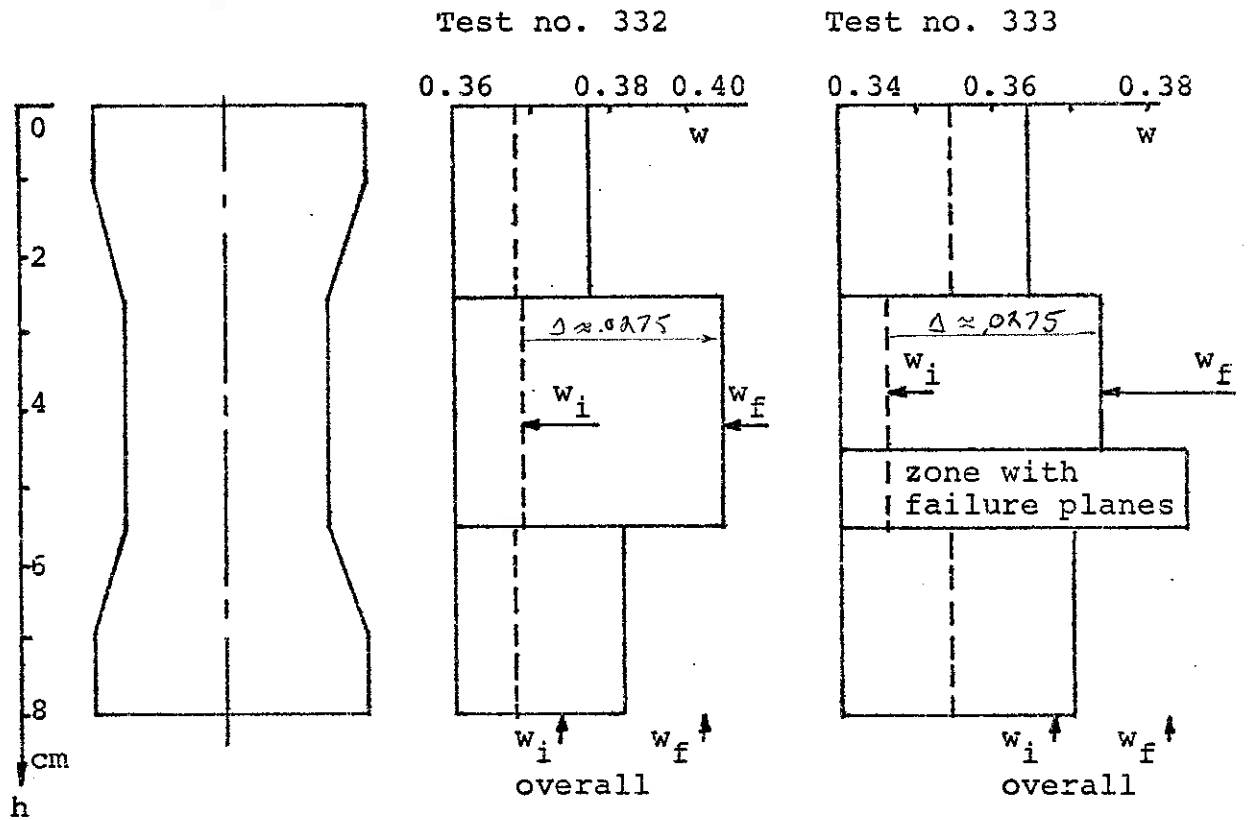
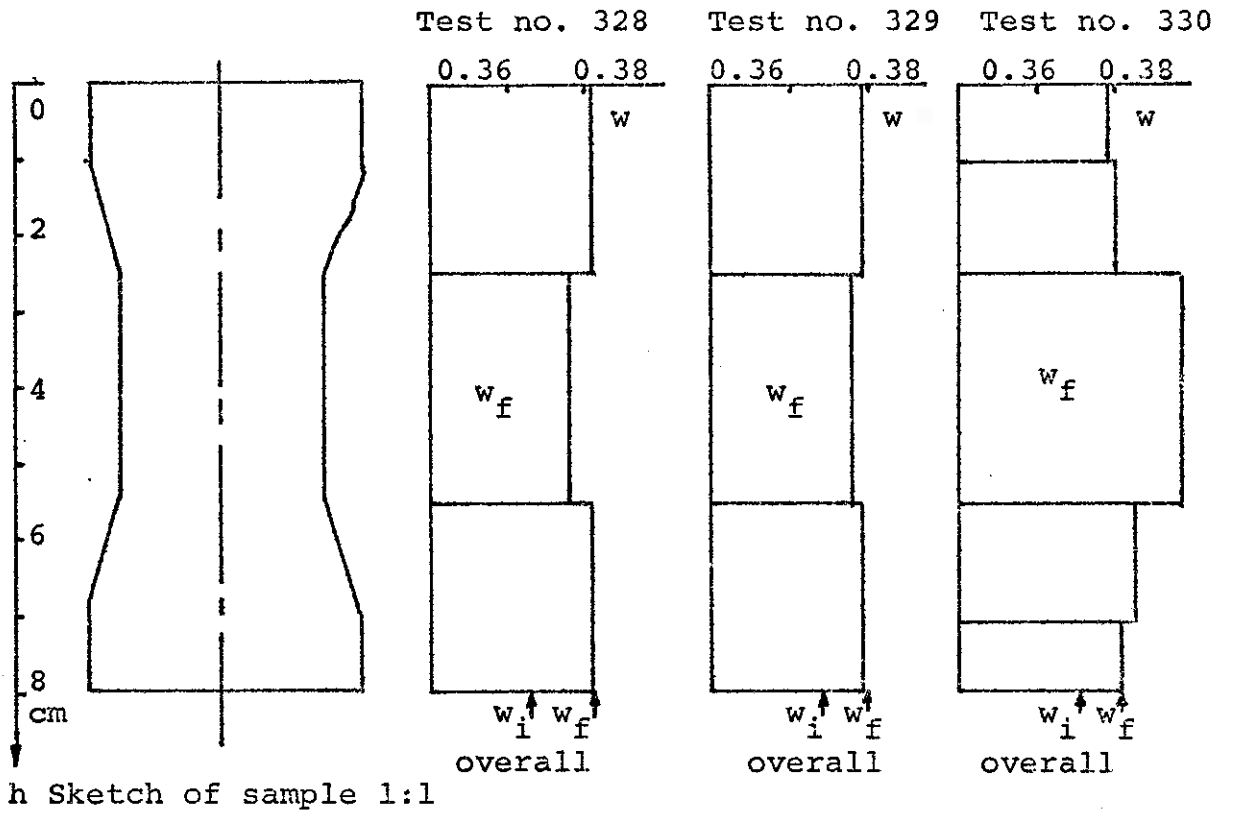


Figure 31. Initial and final water content of specimen

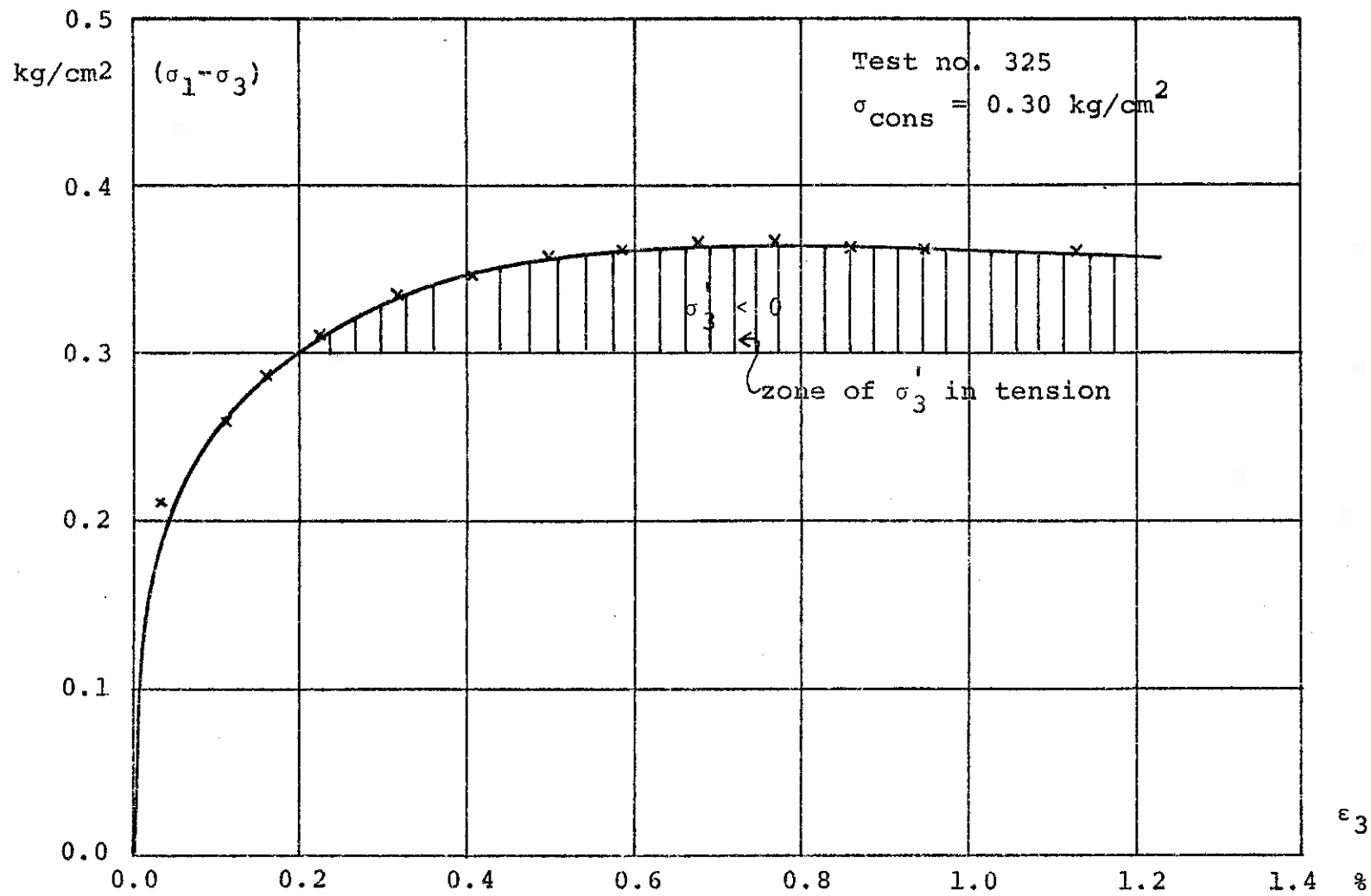


Figure 32. Example of stress-strain curve from test series II

Table 6. Water contents, degrees of saturation and void ratios from test series II: samples

Test No.	Sample No.	$\sigma_{\text{cons}}$ kg/cm <sup>2</sup>	Before test			After cons. phase			After test		
			$w_i$	$S_i$ <i>prob. must corr.</i>	$e_i$	$w_{\text{cons}}$	$S_{\text{cons}}$	$e_{\text{cons}}$	$w_f$	$S_f$	$e_f$
322	22a	0.14	0.374	0.989	0.987	0.380	0.989	1.003	0.385	0.989	1.016
323	23a	0.21	0.364	0.986	0.963	0.369	0.987	0.975	0.371	0.987	0.982
324	25a	0.30	0.374	1.002	0.975	0.379	1.002	0.986	0.379	1.002	0.987
325	27a	0.30	0.377	1.003	0.981	0.376	1.003	0.978	0.378	1.003	0.983
326	28a	0.41	0.375	1.002	0.975	0.374	1.002	0.975	0.375	1.002	0.978
327	29a	0.50	0.375	0.997	0.981	0.375	0.997	0.981	0.375	0.997	0.982
328	31a	0.20	0.374	1.007	0.970	0.378	1.007	0.979	0.380	1.007	0.986
329	32a	0.20	0.375	0.994	0.984	0.377	0.994	0.990	0.379	0.994	0.994
330	33a	0.10	0.375	0.995	0.983	0.381	0.995	0.998	0.387	0.995	1.015
<del>331</del>	<del>34a</del>	<del>0.30</del>	<del>0.369</del>	<del>0.995</del>	<del>0.968</del>	<del>0.265</del>	<del>0.995</del>	<del>0.957</del>	<del>0.371</del>	<del>0.995</del>	<del>0.972</del>
332	36a	0.10	0.373	1.001	0.972	0.380	1.001	0.991	0.389	1.001	1.014
333	37a	0.14	0.366	1.017	0.940	0.370	1.016	0.951	0.377	1.016	0.968

$\bar{\mu} = 0.999$   
 $\sigma = .009$   
 $V = 0.90\%$

$\bar{\mu} = .999$   
 $\sigma = .009$

all same S%

Tops (red)  
Fluorite



**JOHN H. SCHMERTMANN, INC.**

4509 NW 23rd Avenue Suite 19  
 GAINESVILLE, FLORIDA 32606  
 (352) 378-2792  
 FAX (352) 372-9808  
 E-Mail: schmert@ufl.edu

JOB 2030

SHEET NO. \_\_\_\_\_ OF \_\_\_\_\_

CALCULATED BY \_\_\_\_\_ DATE 23 Jul 08

CHECKED BY \_\_\_\_\_ DATE \_\_\_\_\_

SCALE Plot of  $\Delta e$  data, Topsoy p. 64

Table 6

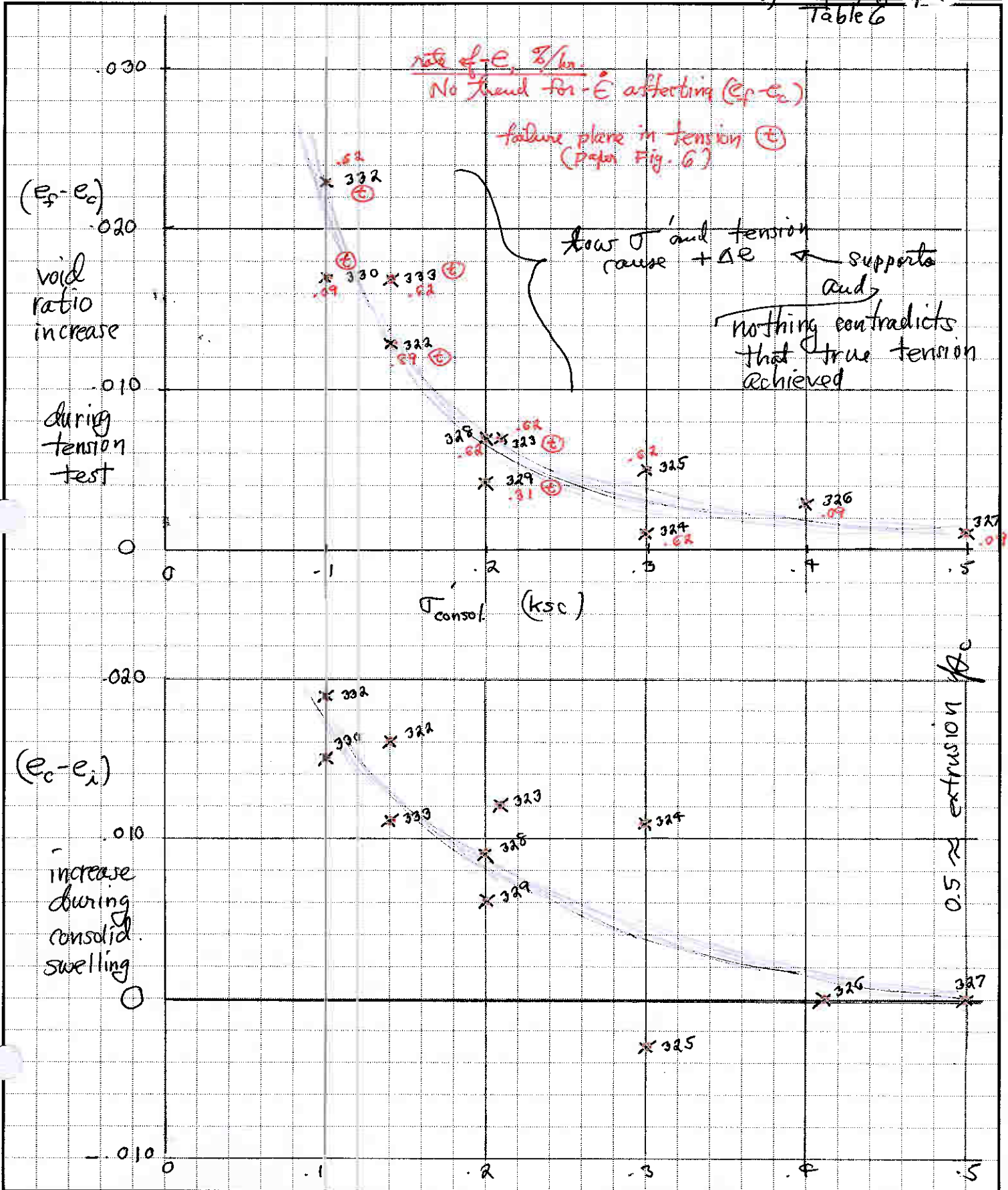


Table 6. Water contents, degrees of saturation and void ratios from test series II: samples

Test No.	Sample No.	$\sigma_{\text{cons}}$ kg/cm <sup>2</sup>	Before test			After cons. phase			After test			
			$w_i$	$S_i$	$e_i$	$w_{\text{cons}}$	$S_{\text{cons}}$	$e_{\text{cons}}$	$w_f$	$S_f$	$e_f$	
322	22a	0.14	0.374	0.989	0.987	0.380	0.989	1.003 <sup>+0.016</sup>	0.385	0.989	1.016	+ .013
323	23a	0.21	0.364	0.986	0.963	0.369	0.987	0.975 <sup>+0.012</sup>	0.371	0.987	0.982	.007
324	25a	0.30	0.374	1.002	0.975	0.379	1.002	0.986 <sup>+0.011</sup>	0.379	1.002	0.987	.001
325	27a	0.30	0.377	1.003	0.981	0.376	1.003	0.978 <sup>-0.003</sup>	0.378	1.003	0.983	.005
326	28a	0.41	0.375	1.002	0.975	0.374	1.002	0.975 <sup>0</sup>	0.375	1.002	0.978	.003
327	29a	0.50	0.375	0.997	0.981	0.375	0.997	0.981 <sup>0</sup>	0.375	0.997	0.982	.001
328	31a	0.20	0.374	1.007	0.970	0.378	1.007	0.979 <sup>+0.009</sup>	0.380	1.007	0.986	.007
329	32a	0.20	0.375	0.994	0.984	0.377	0.994	0.990 <sup>+0.006</sup>	0.379	0.994	0.994	.004
330	33a	0.10	0.375	0.995	0.983	0.381	0.995	0.998 <sup>+0.015</sup>	0.387	0.995	1.015	.017
331	34a	0.30	0.369	0.995	0.968	0.365	0.995	0.957 <sup>+0.019</sup>	0.371	0.995	0.972	
332	36a	0.10	0.373	1.001	0.972	0.380	1.001	0.991 <sup>+0.011</sup>	0.389	1.001	1.014	.020
333	37a	0.14	0.366	1.017	0.940	0.370	1.016	0.951 <sup>+0.011</sup>	0.377	1.016	0.968	.017

$e - e_{\text{cons}}$

Extras.  $\sigma_{\text{ext}} < 1$   
 $\sigma_{\text{ext}} \approx > 0.5$   
 so oc by extr.

## CHAPTER 6

### SERIES III - STRESS-DILATANCY TESTS

#### Introduction

Many investigators have separated their data from shear tests into energy components and strength components. The theory deals with the work which is done by an expanding sample against the surrounding pressure. Different methods, notations and corrections are used by the different investigators. Rowe (19) reviews, compares and discusses the different methods and makes suggestions for the equations which seem to him most relevant. Herein shall only be given a short review of Rowe's thoughts and equations so the basic principle can be understood.

#### Theory

The following notation is used (after Rowe):

$\sigma_1'$  = major principal effective stress

$\sigma_3'$  = minor principal effective stress

$\delta\epsilon_1$  = increment of major principal strain, defined  $\delta\epsilon_1 > 0$   
for compression

$\delta\epsilon_3$  = increment of minor principal strain defined  $\delta\epsilon_3 > 0$   
for compression

$\delta v = 2\delta\epsilon_1 + \delta\epsilon_3$  increment of volumetric strain, defined

$\delta v > 0$  for volume decrease

$\delta E'$  = increment of energy per unit volume transmitted to element

$\delta U$  = increment of internal stored recoverable elastic energy per unit volume

$\delta W$  = increment of energy dissipated per unit volume in frictional heat loss

Subscripts "f" and "corr" refer to the corrected Coulomb's parameters.

For the extension test we have  $\sigma_1 = \sigma_2 > \sigma_3$ . The total energy change per unit volume  $\delta E'$  is divided into two components  $\delta W$  and  $\delta U$ .

$$\delta E' = \delta W + \delta U \quad [18]$$

We have also

$$\delta E' = 2\sigma_1' \delta\epsilon_1 + \sigma_3' \delta\epsilon_3 \text{ (total energy change) } [19]$$

and

$$\delta v = 2\delta\epsilon_1 + \delta\epsilon_3 \quad [20]$$

$$\delta\epsilon_1 = 1/2 (\delta v - \delta\epsilon_3) \quad [21]$$

inserting equation 21 in equation 19 gives

$$\delta E' = \sigma_1' (\delta v - \delta\epsilon_3) + \sigma_3' \delta\epsilon_3 \quad [22]$$

$$\frac{\delta E'}{\delta\epsilon_3} = \sigma_3' - \sigma_1' \left(1 - \frac{\delta v}{\delta\epsilon_3}\right) \quad [23]$$

In equation 18 the term  $\delta U$  is neglected. Bishop and Rowe each has shown that the term  $\delta U$  is small for dense sand. Roscoe has shown that  $\delta U$  is large for normally consolidated clay (19).

In this investigation the elastic component  $\delta U$  is not considered. Only energy  $\delta W$  absorbed in friction will be considered.

This gives

$$\delta E' = \delta W \quad [24]$$

The corrected deviator stress is defined by some investigators by the equation

$$\frac{\delta W}{\delta \epsilon_3} = (\sigma_3' - \sigma_1')_{\text{corr}} \quad [25]$$

for extension. Which gives (equations 24 and 25 in equation 23).

$$(\sigma_3' - \sigma_1')_{\text{corr}} = \sigma_3' - \sigma_1' \left(1 - \frac{\delta v}{\delta \epsilon_3}\right) \quad [26]$$

The modification  $\left(1 - \frac{\delta v}{\delta \epsilon_3}\right)$  applied to  $\sigma_1'$  for an extension test, while for compression Rowe shows with similar equations that the same modification applies to  $\sigma_3'$ . Rowe (19) introduces the modifications in the following form

$$\frac{\sigma_1'}{\sigma_3'}_{\text{corr}} = K_{\text{pf}} = \frac{\sigma_1'}{\sigma_3'} \left(1 - \frac{\delta v}{\delta \epsilon_3}\right) \quad [27]$$

where

$$K_{\text{pf}} = \tan^2 \left(45^\circ + \frac{\phi_f}{2}\right) \quad [28]$$

When an interparticle cohesion  $c_f$  is present  $K_{\text{pf}} + \frac{2c_f}{\sigma_3}$   $K_{\text{pf}}$

replaces  $K_{\text{pf}}$ , as follows:

$$\frac{\sigma_1'}{\sigma_3'} \left(1 - \frac{\delta v}{\delta \epsilon_3}\right) = \tan^2 \left(45^\circ + \frac{\phi_f}{2}\right) + \frac{2c_f}{\sigma_3} \tan \left(45^\circ + \frac{\phi_f}{2}\right) \quad [29]$$

$$\sigma_1' \left(1 - \frac{\delta v}{\delta \epsilon_3}\right) = \sigma_3' \tan^2 \left(45^\circ + \frac{\phi_f}{2}\right) + 2c_f \tan \left(45^\circ + \frac{\phi_f}{2}\right) \quad [30]$$

From the geometry of the Mohr-Coulomb failure, this is equivalent to Coulomb's equation

$$s = c + \sigma \tan \phi \quad [31]$$

The corrected parameters  $c_f$  and  $\phi_f$  can then be found from a  $\tau, \sigma$  stress path by using  $\sigma_1' \left(1 - \frac{\delta v}{\delta \epsilon_3}\right)$  instead of  $\sigma_1'$ , where  $\sigma = \frac{\sigma_1 + \sigma_3}{2}$  and  $\tau = \frac{\sigma_1 - \sigma_3}{2}$ .

Rowe (12) derived the same formula by using the principle of least work. This means the particles move so as to absorb a minimum amount of internal work in friction.

Rowe (12) states the following requirements for the stress-dilatancy tests:

1. The volume changes and strain changes must be measured very carefully.
2. The leakage must be held to a minimum.
3. Constant temperature control within  $\pm 1^\circ\text{C}$ .
4. Rate of testing slow enough to ensure full drainage.
5. Uniform deformation of specimen is necessary, usually requiring frictionless end plates.

The next section describes how these requirements were met. However requirements no. 5 was not met, as there is a filter stone at the bottom of sample and it was thought frictionless end plates could not be used. However, strains to failure were small, perhaps reducing the importance of non-uniform deformations in these tests.

Set up of samples

The same procedure as in test series I was followed in setting up the samples, with a few exceptions. Three internal wool drains were used as in test series I, but the external filter paper strips were not used as drainage aids. To decrease the leakage past the O-rings, four O-rings (internal diameter of 2.9 cm) instead of two were used.

Consolidation

The specimens were consolidated hydrostatically at 1, 2 and 4 kg/cm<sup>2</sup>. Due to air bubble escape, the time for primary consolidation was not obtained for test nos. 334-336. It was found to be 83 minutes for test no. 337 using a drainage pattern of three internal drains and a bottom filter stone. The consolidation phase was left overnight and the extension test was performed the next day.

Performance of tests

The tests were run with a back pressure of 2 or 4 kg/cm<sup>2</sup> and with the cell pressure kept constant. To ensure equilibrium, the back pressure was set on the sample the evening before performance of test. The motor produces heat. To have as little change in temperature as possible during a test, it is best to switch the motor on the day before the test is run and leave it overnight. This was done for test no. 337 only. To ensure full drainage during the first part of test, where

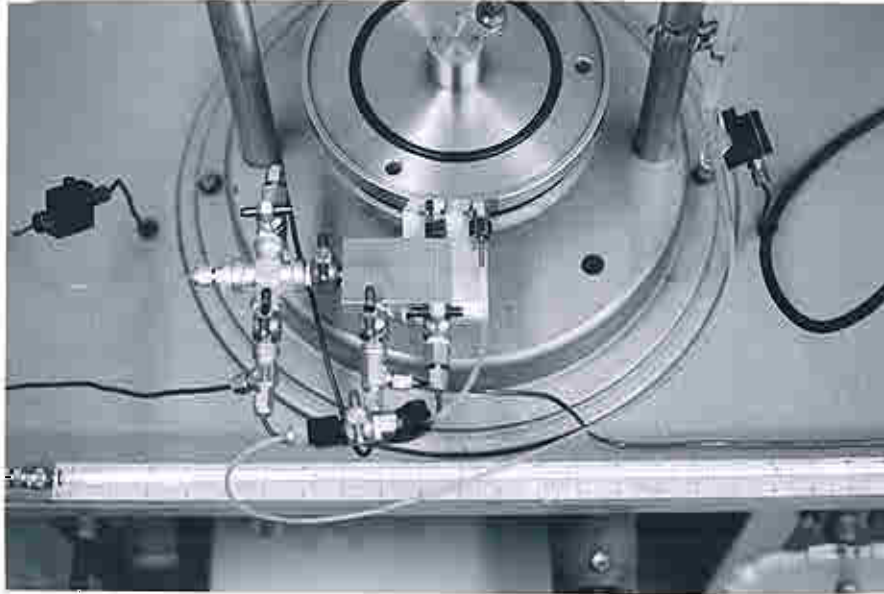


Figure 33. Volume measuring device used in stress-dilatancy tests

By opening two corresponding valves in the valve system, the air bubble in the glass burette will move one way, and by closing the two valves and opening the two other corresponding valves, the air bubble will change direction. In this way, even for large volume changes, the same air bubble can be used throughout the test.



the load increases rapidly, the test was performed very slowly and then the rate of strain was changed from 0.13 to 0.50% per hour after 4-5 hours of testing. It took less than one minute to change the speed; the change caused a sudden increase in deviator stress of about 3.5%.

Readings of simultaneous values of deviator piston load, vertical deformation and volume change was recorded and plotted during each test. The volume of samples 334 and 335 increased during the test, but samples 336 and 337 both increased and decreased. Test no. 336 was stopped before failure because the volume both decreased and increased and an error was suspected. The tests were stopped when the deviator stress reached maximum. After each test, the specimen was measured, and the many diameter measurements showed that the sample deformation appeared very uniform.

For the stress-dilatancy tests the constant temperature condition is very important. The investigator could not control the temperature but only measure it. From measuring the room temperature several times a day, and for one test measuring both room temperature and the temperature in the triaxial cell, it was observed that the cell temperature followed the room temperature, but was all the time about 1°C lower. The variation in temperature was unfortunately up to 5°C during a test day with most of the change in the morning and more constant in the afternoons and evenings. It was noted, however, that the temperature conditions were only this unfavorable for this test series. For test series I and II the temperature was much more constant.

Figure 33 shows the special volume measuring device used in this test series. This device is built entirely of glass and copper, and is therefore very rigid. It is possible to detect volume changes as small as  $0.002 \text{ cm}^3$ . A disadvantage is the many connections and valves, but the system was sensibly leak-free before each test. The back pressure on this burette system was held constant to within  $\pm 0.005 \text{ kg/cm}^2$  by mercury column control to keep the water-air bubble system in volume equilibrium.

### Experimental results

The area of a sample was computed according to the formula  $A = A_0 \frac{1 + \epsilon_v}{1 + \epsilon_3}$ , which is different from the other two test series. The volume change as a function of vertical strain was plotted; from this graph the slope of volume change as a function of strain,  $\frac{\delta v}{\delta \epsilon_3}$  was found. Using a desk computer,  $(1 - \frac{\delta v}{\delta \epsilon_3})$  and the stress-dilatancy corrected values  $\sigma'_1 (1 - \frac{\delta v}{\delta \epsilon_3}) - \sigma'_3$  and  $\sigma'_1 (1 - \frac{\delta v}{\delta \epsilon_3}) + \sigma'_3$  were then calculated. Figure 34 show the stress paths using these corrected values. See Figure 35 for an example stress-strain curve.

The linear regression analysis, least squares, using the desk computer, gave the "cohesion" intercept in Table 7. The "cohesion" intercept was found for different strains.

The change in temperature causes a change in the volume. The change in volume of water in the pores is much greater than the volume increase of the soil solids and the voids,

and having about the same volume, the last two counteract each other. For an increase of  $1^{\circ}\text{C}$  a volume of  $1\text{ cm}^3$  of water will increase  $0.0002\text{ cm}^3$ . With about  $37\text{ cm}^3$  water in the specimen and  $1.5\text{ cm}^3$  in the lines from sample to air bubble, this volume change is equivalent to  $0.32$  inch movement in the volume burette. Because the unknown, but partially compensating, volume expansion of the lines, valves and burette itself were not taken into account, the above is a maximum correction.

The volume change from increase in temperature was added to the volume increase measured. The test data were then recomputed taking the water volume change due to temperature into account. As previously mentioned, the change in temperature was mostly in the morning. This correction is, therefore, only significant at the low strains. See Table 8. The change in temperature might change the test results in other ways, as changes in length or energy changes. This was not taken into account.

For comparison the maximum  $I$  value in test series I was at an average vertical strain of  $2.2\%$  while  $(\sigma_1 - \sigma_3)_{\text{max}}$  in test series II was reached at an average vertical strain of  $1.3\%$ .

There is considerable variation in  $I_0$  ( $\pm 0.552$ ). This may be because the least squares line had to be based on only four points with only two degrees of freedom for the confidence interval. The highest value of bond strength is  $0.117\text{ kg/cm}^2$  at a vertical strain of  $1.9\%$ . A  $95\%$  confidence interval on  $I_0$  gives  $I_0 = 0.117 \pm 0.552\text{ (kg/cm}^2\text{)}$ .

For comparison, it is of interest to note that Ho in his current research has obtained a fundamental cohesion,  $c_f = I_0$ , of only  $0.051 \text{ kg/cm}^2$  from a series of three similar drained compression stress-dilatancy tests on extruded and then overconsolidated kaolinite. Maximum  $c_f$  occurred at a strain of only 0.25%. With these limited data it is uncertain if the difference between  $0.12 \text{ kg/cm}^2$  for extension tests on normally consolidated kaolinite and  $0.05 \text{ kg/cm}^2$  in compression on overconsolidated kaolinite is due to experimental errors or due to theoretical differences between extension and compression tests of this type.

#### Water content, degree of saturation and void ratio

The volume change during consolidation was not obtained due to the many air bubbles. The void ratios and degree of saturation other than the initial values were, therefore, based upon the difference in the final and the initial weight of sample (see Table 9).

#### Conclusion

The 95% confidence interval exceeds the  $I_0 = 0$  intercept. Therefore, there are not enough observations in this test series to conclude whether the extruded kaolinite has a measurable bond strength or a bond strength of zero. For this test series of 4 tests the value of bond strength is  $0.12 \text{ kg/cm}^2$  developed at a vertical strain of 1.9%. However, the 95% confidence interval is a high  $\pm 0.55 \text{ kg/cm}^2$ , making this the least accurate of the three methods compared herein.

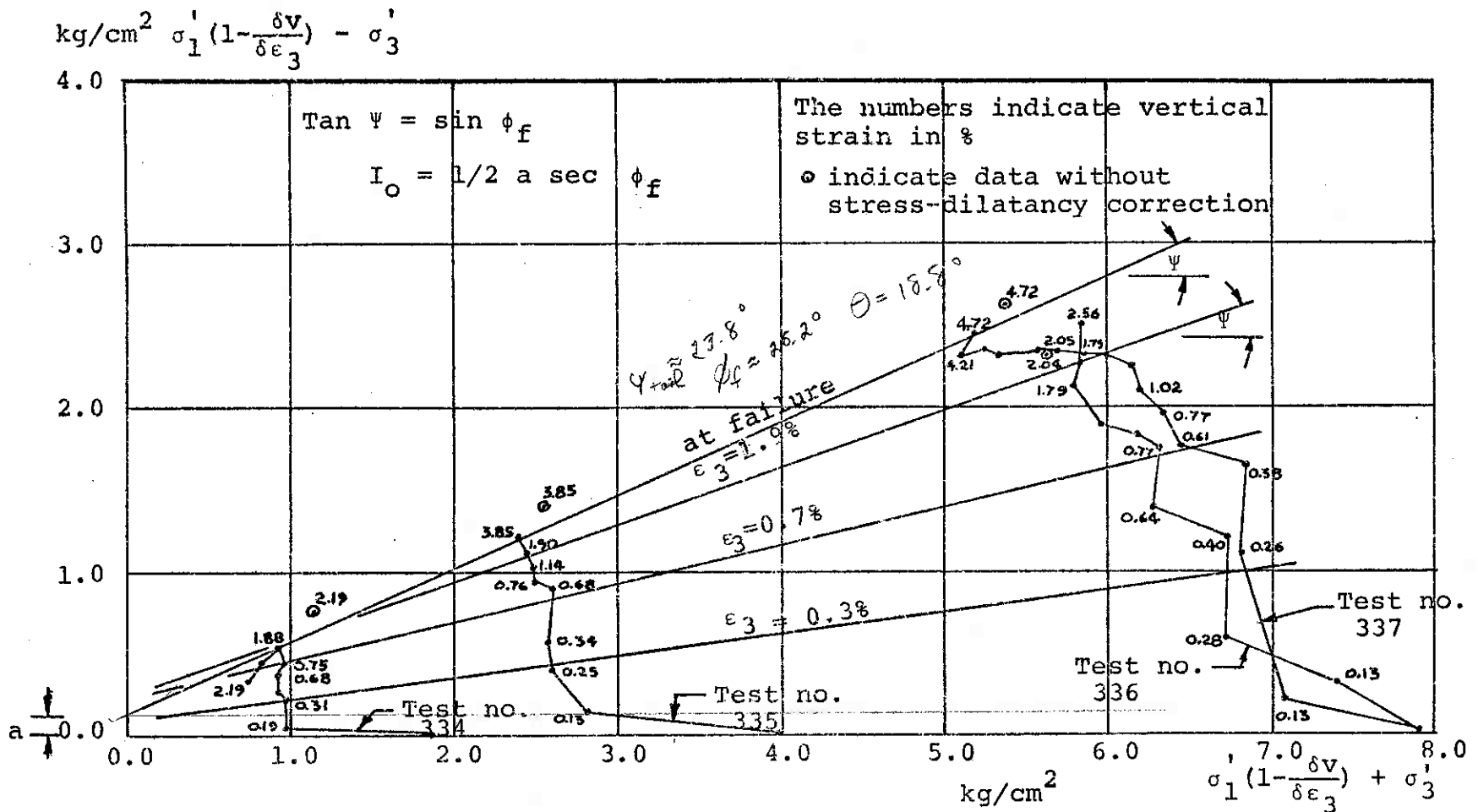


Figure 34. Stress path for test series III with stress-dilatancy correction

Table 7. The "cohesion" intercept from test series III

$\epsilon_3$ %	n no. of obs.	$I_o$ Kg/cm <sup>2</sup>	$I_o$ corr. for temp. change Kg/cm <sup>2</sup>
0.3	4	0.049	0.040
0.7	4	0.114	0.102
1.9	4	0.117	0.117
at $(\sigma_1 - \sigma_3)_{corr, max}$	3	0.071	0.071

Table 8. Results from test series III

Also corrected  
for temp. change

Test No.	$\sigma_1$ Kg/cm <sup>2</sup>	$t_{100}$ min	Back Pressure Kg/cm <sup>2</sup>	Data Point No.	Rate of Strain %/hour	$\epsilon_3$ %	$(\sigma_1 - \sigma_3)$ Kg/cm <sup>2</sup>	$(\sigma_1 + \sigma_3)$ corr Kg/cm <sup>2</sup>	$(\sigma_1 - \sigma_3)$ corr Kg/cm <sup>2</sup>	$(\sigma_1 + \sigma_3)$ corr Kg/cm <sup>2</sup>	$(\sigma_1 - \sigma_3)$ corr Kg/cm <sup>2</sup>
334	0.95	--	4	8	0.13	0.31	0.566	0.976	0.207	0.962	0.193
				13	0.13	0.68	0.667	0.919	0.354	0.905	0.340
				14	0.13	0.75	0.678	0.953	0.409		
				20	0.49	1.88	0.741	0.935	0.517		
				22	0.49	2.19	0.744	0.752	0.341		
335	1.98	--	4	6	0.13	0.25	0.876	2.593	0.385	2.533	0.325
				7	0.13	0.34	0.967	2.573	0.546	2.512	0.485
				10	0.13	0.68	1.126	2.600	0.892	2.540	0.832
				11	0.49	0.76	1.182	2.498	0.902	2.465	0.869
				14	0.49	1.90	1.312	2.438	1.102		
				20	0.49	3.85	1.392	2.391	1.214		
336	3.95	--	4	3	0.13	0.28	0.895	6.696	0.586		
				4	0.13	0.40	1.179	6.721	1.179		
				5	0.13	0.64	1.494	6.265	1.354		
				7	0.49	0.77	1.658	6.317	1.732		
				11	0.49	1.79	2.095	5.805	2.095		
				12	0.49	2.05	2.155	5.838	2.249		
				14	0.49	2.56	2.265	5.822	2.453		
337	3.95	83	2	3	0.13	0.26	1.088	6.812	1.088	6.660	0.935
				4	0.13	0.38	1.332	6.853	1.618	6.701	1.466
				6	0.13	0.61	1.597	6.446	1.739	6.294	1.587
				8	0.49	0.77	1.753	6.337	1.944	6.233	1.839
				12	0.49	1.79	2.166	5.848	2.280		
				13	0.49	2.04	2.230	5.717	2.278		
				22	0.49	4.72	2.567	5.171	2.405		

Test no. 336 was stopped before failure.

Test no. 334

Normally consolidated,  $\sigma_{\text{cons}} = 1.0 \text{ kg/cm}^2$

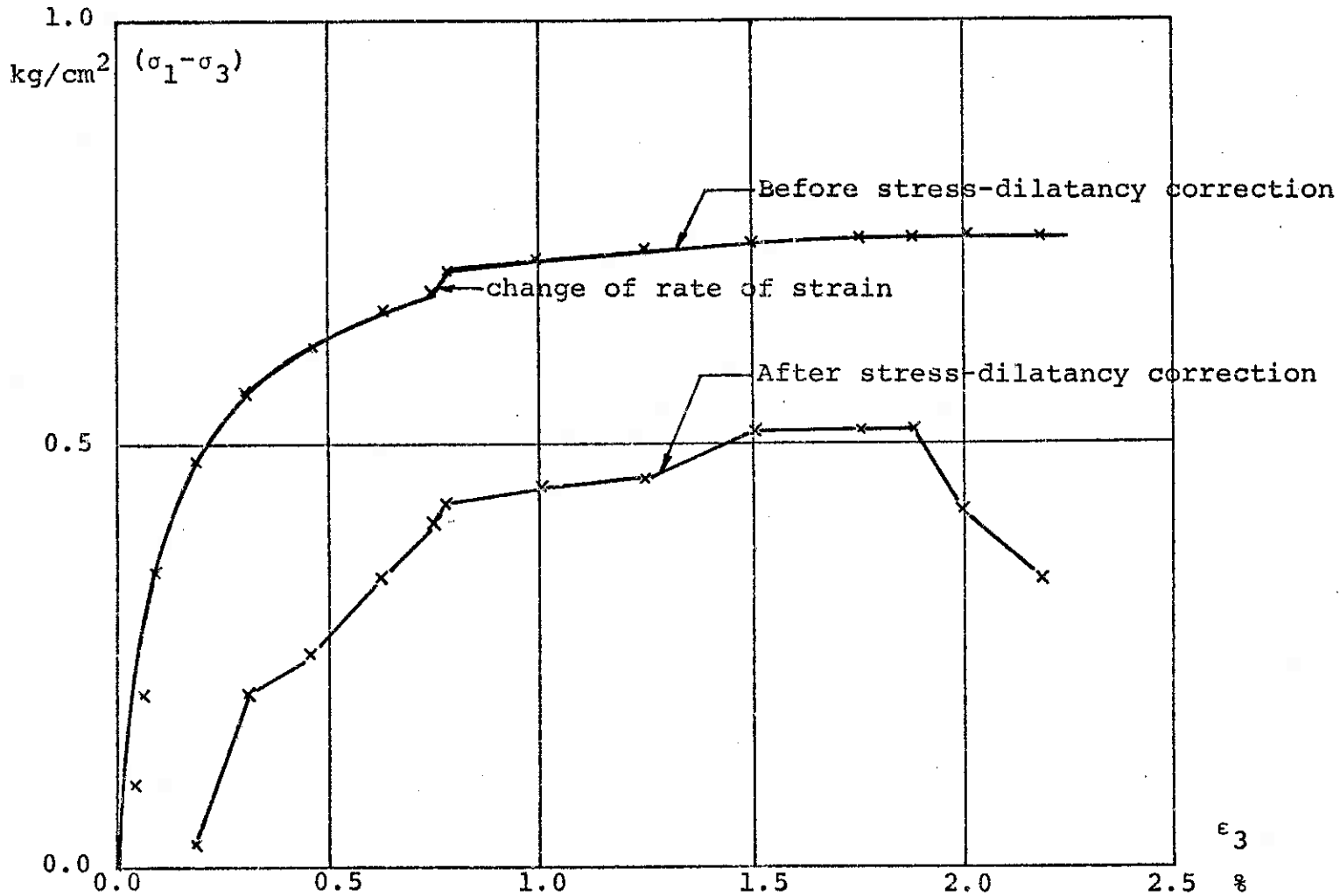


Figure 35. Example of stress-strain curve from test series III



Table 9. Water contents, degrees of saturation and void ratios from test series III samples

Test No.	Sample No.	$\sigma_{\text{cons}}$ Kg/cm <sup>2</sup>	Before test			After cons. phase			After test		
			$w_i$	$S_i$	$e_i$	$w_{\text{cons}}$	$S_{\text{cons}}$	$e_{\text{cons}}$	$w_f$	$S_f$	$e_f$
334	39a	0.95	0.378	0.987	0.999	0.359	0.986	0.950	0.364	0.986	0.962
335	40a	1.98	0.375	0.993	0.985	0.356	0.993	0.936	0.359	0.993	0.944
336	41a	3.95	0.375	0.998	0.981	0.340	0.998	0.889	0.340	0.998	0.882
337	42a	3.95	0.377	0.992	0.992	0.335	0.992	0.881	0.335	0.991	0.881

Table 10. Summary of the measured bond strengths from this investigation

Test Series	Descriptive title	$I_o$ with 95% C.I. Kg/cm <sup>2</sup>	n # of obs
I	IDS tests	0.084 ± 0.025	16
II	Tests on tension samples	0.112 ± 0.041	11
II*		0.084 ± 0.032	11
III	Stress-dilatancy tests	0.117 ± 0.552	4

\* With an approximate stress-dilatancy correction

## CHAPTER 7

### RESUME OF RESULTS AND SUGGESTIONS FOR FUTURE RESEARCH

#### Resume

Table 10 shows a summary of the measured bond strength found in each test series. It is seen that the bond strength is almost independent of method used. Schmertmann found a bond strength of  $0.08 \text{ kg/cm}^2$ , using IDS compression tests on about 50 extruded kaolinite samples in 1966, and Ho found a bond strength of  $0.082 \text{ kg/cm}^2$  for 13 samples also using IDS compression test on extruded kaolinite in 1969. It is concluded that the bond strength of this soil is independent of whether compression or extension testing is used.

An advantage by the IDS test above the other two test series is that stress-dilatancy effects are probably almost absent in the I component determination.

It seems evident that the bond strength of the extruded kaolinite is  $0.08 \text{ kg/cm}^2$ . This investigation confirms further that the bond strength of a soil is a fundamental parameter. Of the three methods tried in this investigation the IDS test is recommended for a determination of a soil's bond strength, because the IDS test has so many advantages. It probably yields the most accurate value, largely because the stress-dilatancy effects are almost absent in the I component.

Furthermore, it was the simplest of the three types of test to perform. It also involves an easily understood theoretical definition, avoiding any theoretical uncertainties in a dilatancy correction.

#### Suggestions for future research

What causes the bond strength? Some investigators have some thoughts and research about the bond strength. The causes could be cementation between particles, viscous forces, electrical forces and/or chemical forces. It would be interesting to investigate some parameters which affect the size of bond strength, perhaps with help of electronic microscopes.

It could be investigated how the theory can be applied in practice or how the bond strength can be related to the bearing capacity of a soil.

## BIBLIOGRAPHY

1. Roscoe, K. H.; Schofield, A. N. and Thurairajah, A. "An Evaluation of Test Data for Selecting a Yield Criterion for Soils," Laboratory Shear Testing of Soils, ASTM Special Technical Publication No. 361, 1963, pp. 111-129.
2. Parry, R. H. G. "Triaxial Compression and Extension Tests on Remoulded Saturated Clays," Geotechnique, Vol. 10, 1960, pp. 166-180.
3. Constantino, C. J. Correspondance, Geotechnique, Vol. 10, 1960, pp. 183-185.
4. Ladd, Charles C.; Varallyay, Julius "The Influence of Stress System on the Behaviour of Saturated Clays During Undrained Shear," U.S. Army Engineer Waterways Experiment Station, CE., Research in Earth Physics, July, 1965.
5. Ladd, Charles C. "Stress-Strain Modulus of Clay from Undrained Triaxial Tests," MIT, Department of Civil Engineering, April, 1964.
6. Kirkpatrick, W. M. "The Condition of Failure for Sands," Proceedings, Fourth International Conference on Soil Mechanics, Vol. I, 1957, pp. 172-178.
7. Bishop, A. W. and Eldin, A. K. G. "The Effect of Stress History on the Relation Between  $\phi$  and the Porosity of Sand," Proceedings, Third International Conference on Soil Mechanics, Vol. I, 1953, pp. 100-105.
8. Habib, M. P. "Influence de la Variation de la Contrainte Principale Moyenne sur la Résistance au Cisaillement des Sols," Proceedings, Third International Conference on Soil Mechanics, Vol. I, 1953, pp. 131-136.
9. Haythornthwaite, R. M. "Mechanics of the Triaxial Test for Soils," Proceedings, Am. Soc. Civ. Engrs., Vol. 86, No. SM 5, 1960, pp. 36-62.
10. Bishop, Alan W. and Henkel, D. J. "The Measurement of Soil Properties in the Triaxial Test," London, 1964.

11. Norges Geotekniske Institut, "Instruction for the Assembly, Maintenance and Use of the Triaxial Equipment Developed at the Norwegian Geotechnical Institute," 1957.
12. Rowe, P. W. ; Oates, D.B. and Skermer, N.A. "The Stress-Dilatancy Performance of Two Clays," Laboratory Shear Testing of Soils, ASTM Special Technical Publication No. 361, 1963, pp. 134-143.
13. Schmertmann, John H. "Generalizing and Measuring the Hvorslev Effective Components of Shear Resistance," Laboratory Shear Testing of Soils, ASTM Special Technical Publication No. 361, 1963, pp. 147-156.
14. Schmertmann, John H. "Comparisons of One and Two-Specimen CFS Tests," Proceedings, Am. Soc. Civ. Engrs., Vol. 88, No. SM6, 1962, pp. 169-206.
15. Schmertmann, J. H. and Osterberg, J. O. "An Experimental Study of the Development of Cohesion and Friction with Axial Strain in Saturated Cohesive Soils," Engineering Progress at the University of Florida, Technical Paper No. 220, 1962.
16. Schmertmann, John H. and Hall, John R. Jr. "Cohesion after Non-Hydrostatic Consolidation," Engineering Progress at the University of Florida, Technical Paper No. 206, 1961.
17. Schmertmann, John H. "The I-Component of a Soil's Shear Resistance," 1966, "A Laboratory Test for Bond Strength," 1966, J. H. Schmertmann's files.
18. Bishop, A. W. and Garga, V. K. "Drained Tension Tests on London Clay," Geotechnique, Vol. 19, 1969, pp. 309-313.
19. Rowe, P.W.; Barden, L. and Lee, I. K. "Energy Component During the Triaxial Cell and Direct Shear Tests, : Geotechnique, Vol. 14, 1964, pp. 247-261.

## BIOGRAPHICAL SKETCH

Miss Anne-Grethe Topshoj was born on November 24, 1943, in Copenhagen, Denmark. In June, 1963, she graduated from the natural sciences line at a Danish high school, Metro-politanskoien. From August, 1963, she studied Civil Engineer- ing at Danmarks Ingeniorakademi in Copenhagen. Following her graduation in January, 1967, she worked at the Danish Geotechnical Institute in the Research Department until June, 1968. From September, 1968, until the present time she has pursued her work at the University of Florida toward the degree of Master of Science in Engineering. She received a graduate research assistantship.

This thesis was prepared under the direction of the chairman of the candidate's supervisory committee and has been approved by all members of that committee. It was submitted to the Dean of the College of Engineering and to the Graduate Council, and was approved as partial fulfillment of the requirements for the degree of Master of Science in Engineering.

June 1970

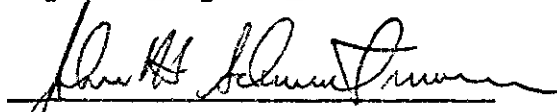
---

Dean, College of Engineering

---

Dean, Graduate School

Supervisory Committee:

  
Chairman

